DOKUZ EYLÜL UNIVERSITY
GRADUATE SCHOOL OF NATURAL AND APPLIED SCIENCES

INVESTIGATING THE BARRIER PERFORMANCE OF GEOSYNTHETIC CLAY LINERS (GCLS) TO CALCIUM CHLORIDE SOLUTIONS IN TERMS OF MASS PER UNIT AREA OF BENTONITE AND NEEDLE PUNCHING DENSITY

by
Fatih POLAT

July, 2022
İZMİR

INVESTIGATING THE BARRIER PERFORMANCE OF GEOSYNTHETIC CLAY LINERS (GCLS) TO CALCIUM CHLORIDE SOLUTIONS IN TERMS OF MASS PER UNIT AREA OF BENTONITE AND NEEDLE PUNCHING DENSITY

A Thesis Submitted to the
Graduate School of Natural and Applied Sciences of Dokuz Eylül University
In Partial Fulfillment of the Requirements for the Degree of Master of Science
in Geotechnical Engineering, Applied Geotechnical Program

by
Fatih POLAT

July, 2022
İZMİR

M.Sc THESIS EXAMINATION RESULT FORM

We have read the thesis entitled **"INVESTIGATING THE BARRIER PERFORMANCE OF GEOSYNTHETIC CLAY LINERS (GCLS) TO CALCIUM CHLORIDE SOLUTIONS IN TERMS OF MASS PER UNIT AREA OF BENTONITE AND NEEDLE PUNCHING DENSITY"** completed by **FATİH POLAT** under supervision of **PROF. DR. ALİ HAKAN ÖREN** and we certify that in our opinion it is fully adequate, in scope and in quality, as a thesis for the degree of Master of Science.

Prof. Dr. Ali Hakan Ören

Supervisor

Assoc. Prof. Dr. Tuğba Eskişar Tefçi

(Jury Member)

Assoc. Prof. Dr. Okan Önal

(Jury Member)

Prof. Dr. Okan Fıstıkoğlu

Director
Graduate School of Natural and Applied Sciences

ACKNOWLEDGEMENTS

First of all, I would like to thank my advisor, Prof. Dr. Ali Hakan Ören, for the support and guidance that he has given me so far. I appreciate him for his support and advice since my undergraduate education. Thanks to him, I learned a lot not only in academic studies but also about humanity. I am grateful for him and I would indicate that I never have accomplished my goals without his support and encouragement.

I have to inform my heartfelt gratitude to my parents and my siblings Mahmut, Emine, Abdurrahman, and Merve Polat for their love and endless support. They have always encouraged me to keep going.

I would like to thank Prof. Dr. Yeliz Yükselen Aksoy, Prof. Dr. Gürkan Özden, Assoc. Prof. Dr. Okan Önal for their contributions and helps throughout my M.Sc study. Also, I have to express my appreciation to Dr. Tuğçe Özdamar Kul for her support and guidance.

I would like to acknowledge my friends, especially Asena Demir Sürer, Nilhan Demirci, İsa Çirkin, Ahmet Yasir Alıcı and Nazım Usta. They have always supported, helped, and encouraged me with their eternal love and patience. I have never forgotten their contributions.

I would like to appreciate my wife, Nihan, who has never left me alone and has endless support. Without her love, I never succeed.

Finally, I would like to thank to the Scientific and Technological Research Council of Turkey (TUBITAK) for the financial support under Grant No: 119R044.

Fatih POLAT

INVESTIGATING THE BARRIER PERFORMANCE OF GEOSYNTHETIC CLAY LINERS (GCLS) TO CALCIUM CHLORIDE SOLUTIONS IN TERMS OF MASS PER UNIT AREA OF BENTONITE AND NEEDLE PUNCHING DENSITY

ABSTRACT

In the content of this study, barrier performance tests were conducted on geosynthetic clay liners (GCLs) to examine the influence of mass per unit area of bentonite (MPUA) and needle-punching density (NPD) on the hydraulic conductivity. In the first part, two types of original GCLs provided by the manufacturer, sodium-bentonite GCL (Na-GCL) and polymer-bentonite GCL (P-GCL), were subjected to tests. The MPUA of original GCLs were 3.0 kg/m^2, 4.0 kg/m^2 and 5.0 kg/m^2. On the other hand, a laboratory type GCL needle-punching apparatus was designed and produced to determine the influence of NPD on the hydraulic conductivity of GCLs. Artificial GCLs (A-GCLs) that have 5, 10 and 15 /cm^2 NPD was produced with the apparatus. To resemble P-GCL, the same type of geotextiles and bentonite were used while manufacturing A-GCLs. Deionized water (DIW) and different concentrations of calcium chloride ($CaCl_2$) solutions were used in the tests. According to the results, the MPUA of GCLs was observed to have a significant effect on the hydraulic conductivity tests when GCLs were permeated with high concentrations of $CaCl_2$ solutions. Especially, MPUA influence the hydraulic breakthrough. That is, hydraulic conductivity of GCLs started to increase later when MPUA increased. The hydraulic breakthrough for the P-GCL was late when compared to Na-GCL. This means that using polymerized bentonite in GCL delay the increase in the hydraulic conductivity. In addition, the influence of NPD on the hydraulic conductivity of GCLs was slightly seen when comparing original GCLs with A-GCLs. As an overall, existence of bundles of fibers are the principal factor that allow increase in the hydraulic conductivity. To overcome their incremental role on hydraulic conductivity, MPUA may be increased furthermore.

Keywords: Geosynthetic clay liner, hydraulic conductivity, mass per unit area of bentonite, needle-punching density, laboratory type GCL needle-punching apparatus.

GEOSENTETİK KİL ÖRTÜLERİN (GKÖ) KALSİYUM KLORÜR ÇÖZELTİLERİNE KARŞI BARİYER PERFORMANISININ BİRİM ALAN BAŞINA BENTONİT KÜTLESİ VE İĞNELEME YOĞUNLUĞU AÇISINDAN İNCELENMESİ

ÖZ

Bu çalışma kapsamında, birim alan başına bentonit kütlesinin (BABBK) ve iğnelenme yoğunluğunun (İY) etkisini incelemek için geosentetik kil astarlar (GKÖ'ler) üzerinde bariyer performans testleri yapılmıştır. İlk bölümde, üretici tarafından sağlanan iki tip orijinal GKÖ, polimer-bentonit GKÖ (P-GKÖ) ve sodyum-bentonit GKÖ (Na-GKÖ), test edildi. Orijinal GKÖ'lerin BABBK'leri testlerde 3.0 kg/m^2, 4.0 kg/m^2 ve 5.0 kg/m^2 idi. Öte yandan, İY'nin GKÖ'lerin hidrolik iletkenliği üzerindeki etkisini belirlemek için laboratuvar tipi bir GKÖ iğneleme aparatı tasarlanmış ve üretilmiştir. Laboratuvar koşullarında aparat ile 5, 10 ve 15 adet/cm^2 İY'ye sahip yapay GKÖ'ler (Y-GKÖ'ler) üretildi. Ayrıca Y-GKÖ'lerin imalatı sırasında, P-GKÖ'lere benzemesi için ile aynı malzemeler (yani geotekstiller ve bentonit) kullanılmıştır. Testlerde deiyonize su (DS) ve farklı konsantrasyonlarda kalsiyum klorür ($CaCl_2$) çözeltileri kullanılmıştır. Sonuçlara göre, GKÖ'lerin BABBK'sinin, yüksek konsantrasyonlarda $CaCl_2$ çözeltileri ile hidrolik iletkenlik testleri üzerinde önemli bir etkiye sahip olduğu gözlendi. Özellikle BABBK, hidrolik atılımı etkiler. Yani GKÖ'lerin hidrolik iletkenliği MPUA arttığında daha geç artmaya başlamıştır. P-GKÖ'de hidrolik atılım, Na-GKÖ ile karşılaştırıldığında geç gerçekleşti. Bu da, GKÖ'de polimerize bentonit kullanılmasının hidrolik iletkenlikteki artışı geciktirdiği anlamına gelir. Ayrıca orijinal GKÖ'leri Y-GKÖ'ler ile karşılaştırdığımızda, İY'nin GKÖ'lerin hidrolik iletkenliği üzerindeki etkisi nispeten görüldü. Genel olarak, lif demetlerinin varlığı, hidrolik iletkenliğin artmasına izin veren başlıca faktördür. Hidrolik iletkenliği arttıran rollerinin üstesinden gelmek için BABBK ayrıca arttırılabilir.

Anahtar kelimeler: Geosentetik kil örtü, hidrolik iletkenlik, birim alan başına bentonite kütlesi, iğnelenme yoğunluğu, laboratuvar tipi GKÖ iğneleme aleti.

CONTENTS

Page

LIST OF FIGURES

Page

LIST OF TABLES

Page

CHAPTER ONE
INTRODUCTION

1.1 Introduction

The rapidly increasing population in the world causes an increase in environmental problems. The municipal solid wastes play an important role in these environmental problems. For this reason, many countries around the world seek solutions to control municipal solid wastes and dispose of them without harming the environment.

Engineers design barrier systems to prevent municipal solid waste from infiltrating and damaging groundwater. Traditionally, compacted clay liners (CCLs) have been used in barrier systems for many years. However, the difficulty of applying CCLs has led to the development of geosynthetic clay liners (GCLs).

GCLs are composite barrier materials that are formed by sandwiching bentonite between two geotextiles (Koerner, 2005; Bouazza and Bowders, 2009). GCLs are widely used as a barrier material because of its low hydraulic conductivity. The thickness of GCLs is between 5-10 mm, and it can be easily installed in the field (Petrov & Rowe, 1997, Jo et al 2001, Ruhl & Daniel, 1997). Thus, GCLs can be used in solid waste storage areas and mining sites in order to prevent the leakage of leachate into the groundwater. Therefore, the barrier performance of GCLs has critical role and numerous chemical and physical factors affect barrier performance of GCLs (Benson et al., 2010; Jo et al., 2005; Katsumi et al., 2008, 2007; Kolstad et al., 2004; Lee and Shackelford, 2005a; Shackelford et al., 2000; Ören and Akar, 2017; Liu et al., 2015; Ören et al., 2019; Rowe et al., 2019, 2017; Chen et al., 2018; Di Emidio et al., 2015; Guyonnet et al., 2005; Mazzieri et al., 2013; Mendes, 2014; Scalia et al., 2014; Setz et al., 2017; Shackelford et al., 2010; Tian et al., 2016; Tong et al., 2021; Wang et al., 2019). In the scope of this study both chemical and physical factors affecting the barrier performance of GCLs have been investigated.

1.2 Scope of the Study

The principal aim of this study is to investigate the influence of mass per unit area (MPUA) and needle punching density (NPD) on the barrier performance of GCLs using calcium chloride solutions ($CaCl_2$) as the permeant.

To manufacture GCL, bentonite is placed within two geotextiles and then those geotextiles are attached each other by needle punching. Although GCLs are manufactured with a target MPUA of bentonite (e.g. 5.0 kg/m^2), MPUA differs throughout the GCL roll, resulting uneven distribution of bentonite. This could happen while manufacturing, transporting or installing the GCL.

GCLs usually have a MPUA of 5.0 kg/m^2. But it is not known where this value come from. Thus, the MPUA of GCL should be determined based on its use on site. For example, low MPUA of GCLs (such as 3.0 kg/m^2) may be sufficient if they are used as cover liners in landfills. Because, GCLs will interact with water and it is well known that bentonite swells when faced with water. On the contrary, high MPUA (i.e. $\geq$ 5.0 kg/m^2) may be preferred if they are used as a barrier material beneath mine tailing ponds or landfills. Increase in the MPUA may increase the hydraulic durability of GCLs. However, this issue has not been investigated so far in detail. But, recent studies showed that the availability of bundles of fibers, which cannot be controlled during manufacturing process, have an important role on the hydraulic conductivity of GCL (Rowe et al., 2019; Rowe & Hamdan, 2021). Inevitably, many bundle of fibers occur on GCLs during manufacturing. However, these bundles do not affect the permeability if GCL is faced with water. Because, the swelling ability of bentonite is perfect against water. However, when bentonite face with leachate, the swelling performance of bentonite decrease and the bundles of fibers act as a hydraulic channel. Hence, hydraulic conductivity may increase in time or even from the beginning.

On the other hand, there is no specific standard for needle-punching density (NPD) when manufacturing GCLs. Just as with MPUA, the NPD of GCLs cannot be controlled. Because hundreds of needles fall on the geotextile with a high frequency.

In addition, it is preferred to use of GCLs with high NPD when peel strength of GCL is important such as use of GCLs on slopes. However, NPD is required not to be high when GCLs are used as a bottom liner or on horizontal surfaces. Since high NPD during manufacturing can create bundles of fibers on GCL, this will negatively affect the permeability of GCLs.

In the scope of this study, the influence of MPUA and NPD was investigated by performing hydraulic conductivity tests on two GCLs (i.e. sodium GCL and polymer treated GCL). Tests were carried out based on three MPUAs (3.0 kg/m^2, 4.0 kg/m^2 and 5.0 kg/m^2). In order to examine the effect of NPD on barrier performance of GCLs, three different NPD was considered (5 $/cm^2$, 10 $/cm^2$, and 15 $/cm^2$). The influence of NPD was assessed on artificial GCLs which had been manufactured in the laboratory with a specially designed GCL needle-punching apparatus. Tests were also performed using calcium chloride solutions ($CaCl_2$) and deionized water (DIW).

CHAPTER TWO
MATERIALS AND METHODS

2.1 Materials

Two GCLs namely sodium bentonite GCL (Na-GCL) and polymer enhanced sodium bentonite GCL (P-GCL) procured from a local manufacturer were used in this study. GCL consists of granular sodium bentonite (Na-Bentonite) and polymer enhanced bentonite (P-Bentonite) which were sandwiched between nonwoven and woven geotextiles by needle-punching. Woven and non-woven geotextiles were used as the carrier and cover geotextiles, respectively.

To categorize the GCLs depending on their MPUA values, numerous GCL specimens in 110 mm diameter were cut from the roll using a mini-fabric cutter. The masses and diameters of these samples were measured and recorded. It was found that the bentonite MPUA values of GCLs were between 2.9 and 6.5 kg/m^2 throughout the roll. The histogram of dry bentonite MPUA of Na-GCL and P-GCL is shown in Figure 2.1a and Figure 2.1b, respectively. Among these GCLs, MPUA with 3.0±0.2, 4.0±0.2, and 5.0±0.2 kg/m^2 were selected and subjected to tests to investigate the influence of MPUA on the hydraulic conductivity of GCLs to $CaCl_2$ solutions. For the simplicity, MPUA with 3.0±0.2, 4.0±0.2, and 5.0±0.2 kg/m^2 will be denoted as M_b3, M_b4 and M_b5, respectively.

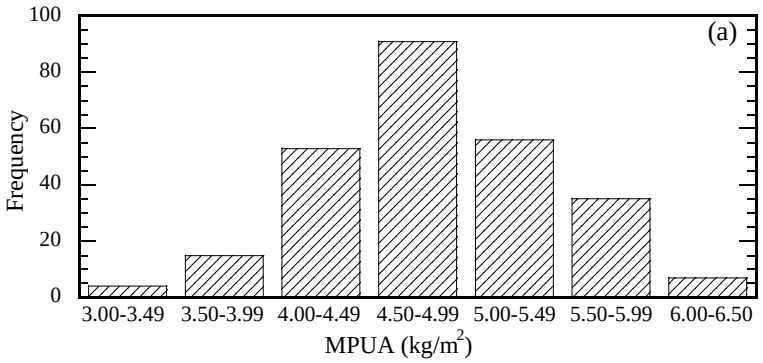

Figure 2.1 Histogram of dry bentonite mass per unit area in the GCLs roll: a) Na-GCL and b) P-GCL

Figure 2.1 Continues

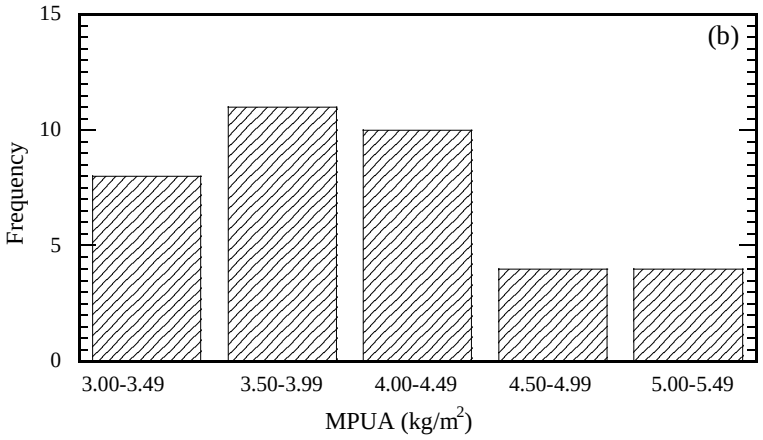

Liquid limit and plastic limit tests were determined on bentonite taken from GCL according to ASTM D4318-17 (2017). The specific gravity test was conducted following the procedure in ASTM D854-14 (2014). The liquid limit, plastic limit, and specific gravity were determined 231%, 61%, 2.70 for Na- Bentonite and 222%, 51%, 2.71 for P-Bentonite. GCL properties are summarized in Table 2.1.

Table 2.1 Geosynthetic Clay Liners (GCLs) Properties

Property	**Na-GCL**	**P-GCL**
Non-Woven Geotextile MPUA (g/m^2)	200	180
Woven Geotextile MPUA (g/m^2)	110	110
Specific Gravity	2.70	2.71
Liquid Limit (%)	231	222
Plastic Limit (%)	61	51
Clay Content (%)	45	70
Swell Index (mL/2g)	21	23.5

Deionized water (DIW) and various concentration of calcium chloride ($CaCl_2$) solutions were used throughout the test program. $CaCl_2$ solutions were prepared by dissolving calcium chloride dehydrate ($CaCl_2 \times 2H_2O$) in DIW. To investigate the influence of $CaCl_2$ concentration on swell index and hydraulic conductivity of GCL, 6.5, 15, 30, and 50 mM $CaCl_2$ solution concentrations were prepared and used in the tests. Since the hydraulic conductivity of Na-GCL to 30 mM $CaCl_2$ solution was high,

it was not needed to performed test with 50 mM $CaCl_2$. In contrast, the hydraulic conductivity of P-GCL to 15 mM $CaCl_2$ solution was low and thus, hydraulic conductivity to 6.5 mM $CaCl_2$ was not determined. Therefore, 6.5, 15, and 30 mM $CaCl_2$ solutions were used when Na-GCL was tested, whereas 15, 30, and 50 mM $CaCl_2$ solutions were used when P-GCL was tested.

2.2 Methods

2.2.1 Sample Preparation

Circular GCL samples were cut from the roll. For this purpose, 110 mm in diameter circles were drawn on the GCL roll. Afterwards these circles were cut using a mini fabric cutter. The diameter and mass of the samples were measured, and their MPUAs were calculated. Then the samples were classified according to their MPUA values. The sample with specified MPUA was selected from that group. Then, the diameter of this group of GCL samples were reduced to 100 mm. The MPUA value of the specimen was recalculated and recorded.

2.2.2 Swell Index Tests

Swell index tests were performed following ASTM D5890-19 (2019). Bentonite was grounded and sieved from No.200 U.S. Standard Sieve (0.075 mm). Before tests, grounded bentonite was dried in an oven at 105°C for 24 hours. Then, 90 mL of testing liquids were filled in 100 mL graduated cylinders. 2.0 g of oven-dried bentonite was poured in the cylinder by 0.1 g increments at 10-minute intervals. Lastly, the additional testing liquid was used to rinse any particles adhering to the sides of the cylinder and to fill the cylinder to 100-mL level. Swell indices were measured and recorded after 24 h.

2.2.3 Hydration Test

Hydration is an important factor for the barrier performance of GCLs. In the field, GCLs expose to hydration and absorb water from the underlying soil. Karakuş et al. (2022) investigated the combined influence of MPUA and subsoil water content on the hydration performance of GCLs. They hydrated GCLs with three different MPUAs (3.0±0.2, 4.0±0.2, and 5.0±0.2 kg/m^2) over compacted silty sand subsoils at various water contents (8, 11, 14, and 17%) up to 180 days. Regardless of MPUA, GCLs reached the maximum water contents after 30 days of hydration.

By considering this situation, GCL specimens were subjected to hydration before hydraulic conductivity tests using flexible wall permeameters. For this purpose, GCL specimens with 100 mm in diameter and with M_b3, M_b4 and M_b5 were hydrated with DIW up to 72h under 35 kPa cell pressure. The inflow port of the permeameter was kept open and the outflow port was closed during hydration. To determine the water content-time relationship, GCLs were removed from the permeameters after 4, 24, and 48h of hydration. The wet mass of GCLs were weighted and then they placed into the permeameter cells to continue for the hydration. Finally, permeameters were dismantled at the end of 72h of hydration, samples were weighted and then dried in an oven at 105 ºC to calculate the dry mass of GCLs. The GCL water contents were calculated by dividing the mass of water to dry mass of GCLs.

Figure 2.2 shows the water uptake of GCLs during hydration. Karakuş et al. (2022) also used the same GCLs with similar MPUA range for the hydration. However, they hydrated the GCLs over compacted silty sand for 30 days. Thus, the range of final water contents reported in their study was represented with a hatched zone as shown in Figure 2.2.

The water contents of GCLs rapidly increased to 122% for M_b3, 105.5% for M_b4 and 85.2% for M_b5 in the first 4h of hydration. The rate of change in the water contents remarkably decreased in the following hydration step (i.e. 24h). The water contents of GCLs for M_b3, M_b4 and M_b5 reached to 145.1%, 135.5%, and 119% after 24h,

respectively. Then, the final water content increased to 165.1%, 135.5%, and 119% after 72h of hydration, respectively. It is obvious that the higher the MPUA the lower is the final water content of GCLs. This conclusion is in agreement with the previous results reported in the literature which determine the hydration behavior of GCLs over compacted subsoils (Rayhani et al., 2011; Anderson et al., 2012; Sarabian and Rayhani, 2013; Karakuş et al., 2022; Ören et al., 2022). By comparing the hatched zone in Figure 2.2, applying 4h hydration duration to GCLs before commencing the hydraulic conductivity tests seemed to be adequate. However, since preparing the GCL for the hydraulic conductivity test is a time consuming process and the hydraulic conductivity performance of GCL should be monitored at the beginning of the permeation for a while, it was decided to apply 24h for the hydration.

Since the availability of flexible wall permeameters were limited, the hydration performance of GCLs were only determined using DIW. Thus, the same hydration duration was applied when the hydraulic conductivity tests were carried out with $CaCl_2$ solutions.

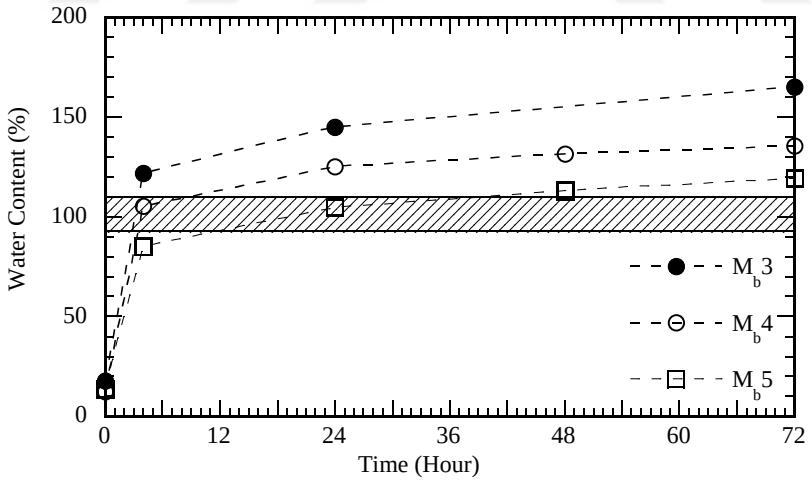

Figure 2.2 Influence of hydration on the GCL water content

2.2.4 Hydraulic Conductivity Tests

The falling head constant tail water method described in ASTM D:6766-12 was used during the hydraulic conductivity tests. Instead of porous stones, GCLs were sandwiched between two heavy non-woven geotextiles, and the perimeters of the GCLs were sealed with bentonite taken from the roll. Then, latex membrane was placed over the GCL and three O-rings were attached on top and bottom pedestals. After placing samples in permeameter cells, permeameters were filled with tap water. Tests were performed under 35 kPa effective stress and an average hydraulic gradient of 35. DIW and $CaCl_2$ solutions with various concentrations (i.e. 10, 20, 50 mM) were used as the permeants. The flow direction was from top to bottom. Before the flow was initiated, GCLs were hydrated with the permeant solutions for 24h.

Hydraulic conductivity tests with $CaCl_2$ solutions were continued until establishing the pH and EC equilibrium between the influent and effluent solutions (ASTM D6766-12, 2012). Equilibrium in pH and EC was achieved when the effluent pH and EC were within ±10% of the influent solution. In this study, hydraulic conductivity tests were mostly terminated after pH and EC equilibriums were established.

2.2.5 Chemical Analysis

2.2.5.1 pH and Electrical Conductivity Measurements

At specific time intervals, liquid samples were collected from inflow and outflow port of permeameter cells. Then, pH and electrical conductivity (EC) were measured on these influent and effluent samples using accumet XL 500 benchtop meter. Before measuring, probes were calibrated with related buffer solutions.

2.2.5.2 Bound Cation Determination

The bound cation tests were performed on bentonites extracted from each GCL following ASTM D7503-18. Tests were conducted with 10 g air dry bentonite and 1

M ammonium acetate (NH4OAc) solution. First, 10 g bentonite and 40 mL NH4OAc were mixed in a plastic bottle, and the suspension was shaken with an end over shaker at 30 rpm for 5 min. After 24h curing, the suspension was shaken again for 15 min at 30 rpm. After that, the suspension was filtered through Whatman No 42 ashless filter paper in the Buchner funnel. Bentonite was washed four times with 30 ml of NH4OAc and applied <10 kPa vacuum pressure during filtering. Then, the bound cations of the filtrates were determined using inductively coupled plasma optical emission spectrophotometry (ICP-OES).

CHAPTER THREE
INFLUENCE OF MPUA ON THE BARRIER PERFORMANCE OF GCLs

3.1 Background

Geosynthetic clay liners (GCLs) are composite barriers which are used for their containment function. Bentonite is sandwiched between two geotextiles by needle punching, adhesive, or stitch bounding. The containment ability of GCLs is satisfied by the bentonite. Sodium (Na^+) and calcium (Ca^{2+}) as well as polymerized (i.e. polymer loaded) bentonite is used to achieve lower hydraulic conductivity for the GCLs. Therefore, the efficacy of a GCL mostly depend on the quality of bentonite component.

Bentonite is abundant of montmorillonite type of clay mineral and thus, it has high swelling potential (Lee et al, 2005). The swelling potential of bentonite depends on the type of cations present in the exchangeable site of molecular structure. Sodium (Na^+) bentonite is generally used in GCLs which has high swelling potential. High swelling potential results in low pore spaces available for mobile water and gives low permeability. Therefore, Na-GCL has lower hydraulic conductivity than GCLs containing Ca^{2+} rich bentonites.

On the other hand, GCLs exposed to cation exchange during hydration and permeation in the field. The monovalent cations in GCLs replace with divalent and trivalent cations present in subgrade soil or permeant liquids. This cation replacement causes a significant effect on the hydraulic performance of GCLs. That is, the swelling ability of GCL decreases with the cation replacement, and hence its hydraulic conductivity increases (Jo et al, 2004).

Several studies have simulated how the cation exchange occurred during hydraulic conductivity tests when permeated with synthetic or actual municipal solid waste leachates (Jo et al, 2001, Lee and Shackelford, 2005, Benson et al, 2010). These studies have shown that permeation with weak solutions ($\leq$ 20 mM) gives comparable

hydraulic conductivities to those obtained with deionized or tap water. In contrast, these studies also showed that using strong solutions (≥ 50 mM) with multivalent cations as a permeant caused high hydraulic conductivity values (> 1.0×10^{-9} m/s). However, none of these studies evaluated the hydraulic performance of GCLs based on the bentonite mass per unit area (MPUA).

MPUA refers to the amount of dry bentonite corresponding to the unit area of GCL. During the manufacturing process, GCLs often have uneven bentonite distribution throughout the rolls. This uneven distribution causes variation in the MPUA. In other words, MPUA values are somewhat different throughout the roll of the GCL. The hydraulic conductivity of GCL may show some differences depending on the MPUA values. Limited studies have investigated the influence of MPUA on the barrier performance of GCLs (Salemi et al 2018, Rowe et al. 2017). However, the primary concern of previous studies were not MPUA and none of these studies were extensively examined the influence of MPUA on the hydraulic conductivity. As there is scarce information about the influence of MPUA on the barrier performance of GCLs, it deserves more attention to detail.

Since the hydraulic conductivity of GCLs increase with salt solutions, most of the studies reported in the literature basically carried out using $CaCl_2$ solutions (Jo et al., 2001, Kolstad et al., 2004; Lee and Shackelford, 2005a; Katsumi et al., 2008; Bohnhoff & Shackelford, 2013; Rowe & Li, 2020). Calcium has two valences and the thickness of diffuse double layer surrounding the bentonite particles decrease as the valence of cation increase (Mitchell & Soga, 2005). Thus, a brief literature will be given herein which are related to the performance evaluation of GCLs against salt solutions. Then, literature regarding to MPUA will be given.

3.1.1 Influence of Salt Solutions on the Swell Index and Hydraulic Conductivity of GCLs

Jo et al. (2001) examined the influence of single-species salt solutions on the free swell and hydraulic conductivity of GCLs. They used different salt solutions (i.e.

$CaCl_2$, NaCl, KCl, $MgCl_2$) which had monovalent, divalent, and trivalent cations during the tests. They showed that the hydraulic conductivity increased and swell indices of bentonite decreased when concentrations of salt solutions increased.

Jo et al. (2005) also conducted long-term hydraulic conductivity tests on two types of GCLs with salt solutions. They used both weak (5, 10, and 20 mM) and strong (50, 100, and 500 mM) $CaCl_2$ solutions as the permeants. Hydraulic conductivities were initially low and then increased significantly, when weak $CaCl_2$ solutions were used. The reason for this increase was attributed to the cation replacement that took place between permeant and GCL during the permeation. Furthermore, high hydraulic conductivity values ($>10^{-9}$ m/s) were obtained for both GCLs when strong $CaCl_2$ solutions were used. As a result, the final hydraulic conductivity increased as the $CaCl_2$ concentration increased.

Katsumi et al. (2008) investigated the long-term barrier performance of two bentonites (i.e. natural bentonite (NB) and multiswellable bentonite (MSB)) and two GCLs against NaCl and $CaCl_2$ solutions. They concluded that the hydraulic conductivity of GCLs significantly correlated with the swell indices of bentonites. The bentonites that have greater swell indices than 20 mL/2g gave lower hydraulic conductivities ($< 1.0\times10^{-10}$ m/s).

Tian et al. (2019) conducted hydraulic conductivity and free swell tests on two bentonite polymer composite GCLs. They used DIW and $CaCl_2$ solutions as the reagent water in the experiments. Regardless of the bentonite type, they showed that the swell indices decrease as the $CaCl_2$ concentration increase. In contrast, the hydraulic conductivities of GCLs increased with an increase in the $CaCl_2$ concentration.

Wireko and Abichou (2021) investigated physicochemical factors that influence polymer elution from the GCLs. They performed hydraulic conductivity and swell index tests on two GCLs with DIW and $CaCl_2$ solutions. DIW and 5, 10, 20, 50, 100, 200, and 500 mM $CaCl_2$ solutions were used as the reagent water for the free swell

tests, whereas the hydraulic conductivity tests were conducted with DIW and high concentrations of $CaCl_2$ solutions (50, 200, and 500 mM). The swell indices decreased as the $CaCl_2$ concentration increased from 5 to 500 mM. GCLs had low hydraulic conductivities with DIW (3.7×10^{-12} and 2.0×10^{-11} m/s). In contrast, high hydraulic conductivities (> 1.0×10^{-9} m/s) were obtained for both GCLs with high concentration of $CaCl_2$ solutions.

3.1.2 Influence of MPUA on the Hydraulic Conductivity of GCLs

Von Maubeuge and Ehrenberg (2014) investigated the minimum MPUA requirement for the GCLs. They conducted index flux, permittivity and hydraulic conductivity tests on GCLs with various MPUAs. In the content of their study, GCLs samples with MPUA ranging between 3.0 and 8.0 kg/m^2 were permeated with water. They showed that the permeability slightly decreased or stayed nearly constant with an increase in the MPUA. In addition, they concluded that the range of hydraulic conductivity data was low when MPUA was high.

Rowe et al. (2017) performed hydraulic conductivity tests on exhumed GCLs that were in service for 5 and 7 years in a cover. They investigated the hydraulic conductivity behavior of four exhumed GCLs with MPUA ranging between 4.5 and 6.0 kg/m^2 under different conditions. They used 10 mM $CaCl_2$ solution as the permeant for the hydraulic conductivity tests. According to the test results, the hydraulic conductivity of GCL with lower MPUA (4.5 kg/m^2) was 100 times greater than the hydraulic conductivity of GCL with higher MPUA (6.0 kg/m^2) (2.0×10^{-7} m/s versus 2.0×10^{-9} m/s). The results indicated the influence of MPUA on the hydraulic conductivity of GCLs with $CaCl_2$ solutions. However, the influence of MPUA was investigated in a narrow range in their study.

Salemi et al. (2018) investigated the influence of some structural parameters on the hydraulic performance of GCLs with MPUA of 3.0, 4.0 and 5.0 kg/m^2. GCLs that have nonwoven geotextiles on both sides were used in the experiments. The hydraulic conductivity test results showed that the permeability of the GCLs with 4.0 and 6.0

kg/m^2 MPUA were 2.1×10^{-7} and 1.5×10^{-7} m/s, respectively. They concluded that the hydraulic conductivity of GCLs slightly decreased when MPUA increased from 4.0 to 6.0 kg/m^2.

This study discusses hydraulic conductivity tests conducted on Na-GCL and P-GCLs with different MPUAs (ranging between 3.0 and 5.0 kg/m^2) to $CaCl_2$ solutions (6.5, 15, 30, and 50 mM). The objective of this study is to evaluate the combined infleunce of MPUA and permeant concentration on the barrier performance of GCLs. The swell index tests and chemical analyses were also conducted on the GCLs.

3.2 Influence of MPUA on the barrier performance of Na-GCLs

3.2.1 Swell Index

The swelling ability of Na-bentonite in DIW and $CaCl_2$ solutions are quantified in terms of swell index (SI) values. Figure 3.1 shows the change of SI with the $CaCl_2$ solution. The SI of Na-Bentonite in DIW was 21 mL/2g. Then, SI decreased to 18, 13, and 10.5 mL/2g in 6.5, 15 and 30 mM $CaCl_2$ solutions. The results showed that the reagent water (or pore fluid) had a significant effect on the swelling ability of bentonite. The reduction in the SI values are due to the divalent cation present in $CaCl_2$ solutions (Lee et al, 2005). Na^+ cations available in the exchangeable sites of bentonite replaced with Ca^{2+} cations present in the solutions, resulting the suppression of diffuse double layer surrounding the bentonite particles. Since the thickness of diffuse double layer is inversely related with the concentration and valence of the cation (Sridharan et al., 1986; and Jo et al., 2001), the greatest decrease in SI was obtained when $CaCl_2$ concentration was 30 mM.

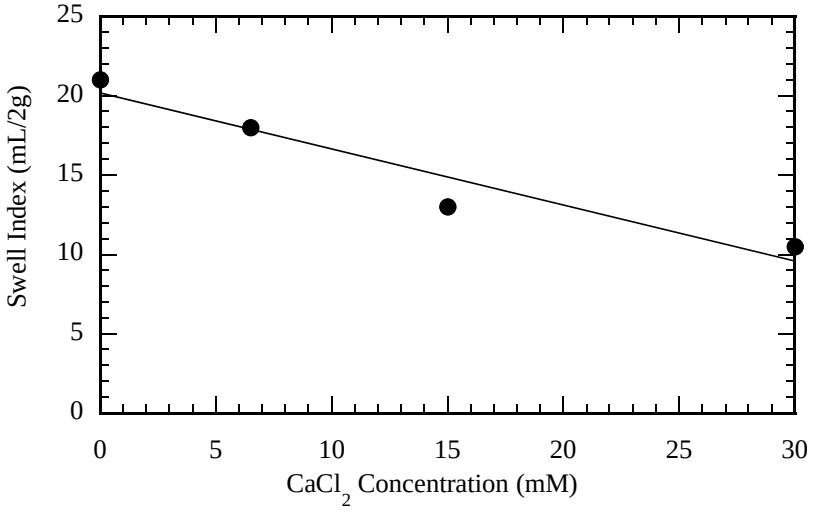

Figure 3.1 Swell indices of Na-Bentonite in DIW and $CaCl_2$ solutions

3.2.2 Hydraulic Conductivity of Na-GCLs

Hydraulic conductivity tests were performed on the Na-GCLs with M_b3, M_b4, and M_b5 using DIW and $CaCl_2$ solutions. Final hydraulic conductivity values were calculated by taking the average of the last four consecutive readings and are summarized in Table 3.1. As presented in Table 3.1, hydraulic conductivities of M_b3, M_b4 and M_b5 to DIW are close to each other, but slightly increased from 2.1×10^{-11} to 4.6×10^{-11} m/s as the MPUA decreased. On the other hand, the hydraulic conductivities of GCLs with $CaCl_2$ solutions changed depending on the MPUA and the concentration of $CaCl_2$ solutions (Table 3.1).

Table 3.1 The Final Hydraulic Conductivities of Na-GCLs to DIW and $CaCl_2$ Solutions.

Test Number	Measured MPUA (kg/m^2)	Denotation of GCLs	Permeant	Duration (days)	PVF	Hydraulic Conductivity (m/s)
1	3.07	M_b3	DIW	118	8.8	4.6×10^{-11}
2	3.08	M_b3	6.5 mM $CaCl_2$	4.5	20	3.4×10^{-9}
3	3.08	M_b3	15 mM $CaCl_2$	0.6	31	7.6×10^{-8}
4	3.10	M_b3	30 mM $CaCl_2$	0.5	28	1.3×10^{-7}

Table 3.1 Continues

5	4.13	M_b4	DIW	165	5.1	2.9×10^{-11}
6	4.02	M_b4	6.5 mM $CaCl_2$	409	11	2.3×10^{-11}
7	4.03	M_b4	15 mM $CaCl_2$	187	33	2.8×10^{-9}
8-a	4.05	M_b4 (Test 1)	30 mM $CaCl_2$	2.9	37	4.3×10^{-8}
8-b	4.08	M_b4 (Test2)	30 mM $CaCl_2$	10	31	2.5×10^{-8}
8-c	3.94	M_b4 (Test 3)	30 mM $CaCl_2$	8.2	33	2.4×10^{-8}
9	4.85	M_b5	DIW	191	6.1	2.1×10^{-11}
10	4.99	M_b5	6.5 mM $CaCl_2$	440	12	2.1×10^{-11}
11	5.07	M_b5	15 mM $CaCl_2$	288	37	1.5×10^{-8}
12-a	4.88	M_b5 (Test 1)	30 mM $CaCl_2$	5.6	27	8.3×10^{-9}
12-b	5.03	M_b5 (Test 2)	30 mM $CaCl_2$	170	40	8.2×10^{-9}

3.2.3 Hydraulic Conductivity of Na-GCLs to 6.5 mM $CaCl_2$ Solutions

The hydraulic conductivity of Na-GCLs to 6.5 mM $CaCl_2$ solutions is given in Figure 3.2a as a function of pore volume of flow (PVF). The hydraulic conductivity of M_b3 was initially high (i.e. 1.0×10^{-7} m/s) and then slightly decreased to 3.4×10^{-9} m/s throughout the test. The initial hydraulic conductivity of M_b3 was high because preferential flow paths occurred through the gaps between the aggregates and bundle of fibers. Since bentonite exhibited appreciable amount of swelling in 6.5 mM $CaCl_2$ solution (Figure 3.1), Na-bentonite started to swell laterally and close the gaps between the aggregates. Hence, hydraulic conductivity reduced about 30 times when compared to the initial. However, the final hydraulic conductivity of M_b3 is still greater than that of M_b4 and M_b5 (3.4×10^{-9} vs. 2.2×10^{-11} m/s). This shows that bundle of fibers in M_b3 still possessed preferential flow paths even bentonite swollen laterally.

The pH and EC values of effluents are drawn in Figures 3.2b and 3.2c, respectively. The influent pH and EC values are also shown with dashed lines on the same Figures. The pH of M_b3, M_b4 and M_b5 were almost constant throughout the tests and around

9.3±0.3 (Figure 3.2b). The influence of MPUA on the pH values of effluents cannot be seen during the permeation with 6.5 mM $CaCl_2$. In contrast, the EC of effluent showed a decreasing trend during permeation. Although the decreasing trend in EC was similar for all GCLs, EC lines differs from each other depending on the MPUA (Figure 3.2c). The EC values of M_b3 was measured almost two times lower than that of M_b4 and M_b5. Since hydraulic conductivity was high for this GCL, the solution had limited time to react with bentonite during permeation. Thus, the EC values of M_b3 were close to EC influent line. In contrast, EC values for M_b4 and M_b5 were high with respect to M_b3, when the hydraulic conductivity tests were terminated. This is possibly due to incomplete cation replacement between GCLs and the permeant. Figure 3.2d and 3.2e also show that cation replacement was still in progress for M_b4 and M_b5 at the time of termination which means that effluent still contains appreciable amount of Na^+ extracted from bentonite. Thus, the EC values of M_b4 and M_b5 was found greater than M_b3.

The effluent cation concentrations of M_b3 were not measured, because it did not satisfy the barrier property in terms of hydraulic conductivity (Figure 3.2a). Thus, Figure 3.2d and Figure 3.2e show the effluent concentrations just for M_b4 and M_b5. The effluent Na^+ and Ca^{2+} concentrations of M_b4 and M_b5 were similar to each other as in their hydraulic conductivities. The effluent Na^+ concentrations for M_b4 and M_b5 continued to decrease (Figure 3.2d), whereas Ca^{2+} concentrations slightly increased after ~400 days of permeation with 6.5 mM $CaCl_2$ solution. This shows that extensive test durations should be applied to reach the chemical equilibrium, when such a low $CaCl_2$ concentration is used. However, due to time restrictions, the hydraulic conductivity tests for both GCLs must have been terminated before the chemical equilibrium was established.

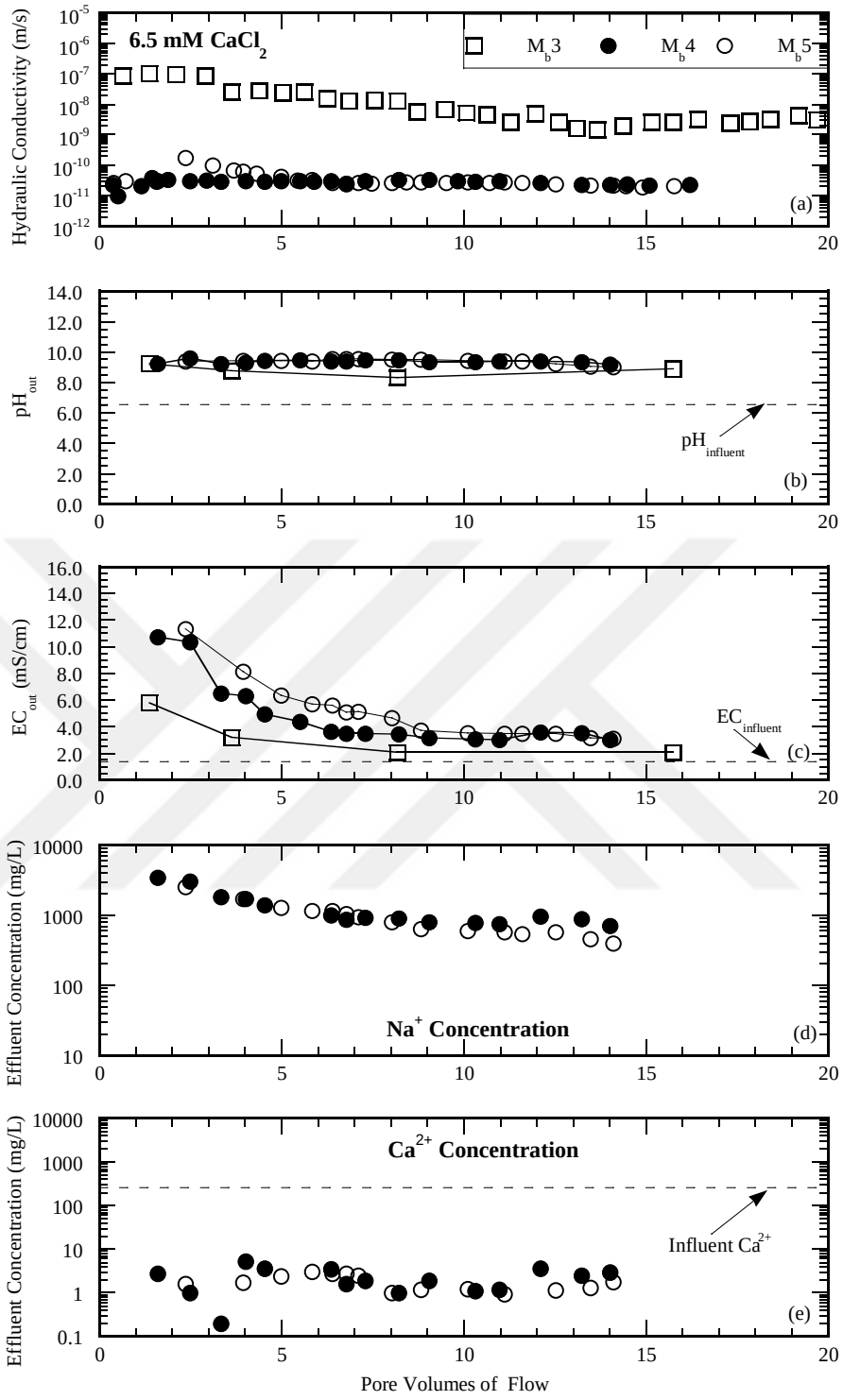

Figure 3.2 a) Hydraulic conductivity behaviors of Na-GCL with M_b3, M_b4 and M_b5 to 6.5 mM $CaCl_2$ solution, and b) pH, c) electrical conductivity (EC), d) sodium (Na^+), and e) calcium (Ca^{2+}) concentrations of influent and effluent

3.2.4 Hydraulic Conductivity of Na-GCLs to 15 mM $CaCl_2$ Solutions

Hydraulic conductivity behaviors of M_b3, M_b4, and M_b5 to 15 mM $CaCl_2$ solutions as well as pH, EC, Na^+ and Ca^{2+} concentrations measured in the influent and effluents are drawn as a function of PVF and shown in Figure 3.3a-e. The hydraulic conductivity of M_b3 was almost constant and around 7.6×10^{-8} m/s throughout the test duration (Figure 3.3a). At the end of the hydraulic conductivity test, a dye test was conducted on M_b3 to determine if there were any preferential flow paths occurred across the sample. The woven geotextile was separated from the GCL using a razor knife to clearly observe potential flow paths on swollen bentonite (Figure 3.5). As seen from Figure 3.5, pink dyed regions show the bundle of fiber induced flow paths across the GCL. Since both the amount of bentonite in M_b3 and swell index in 15 mM $CaCl_2$ solution were low (i.e. 13 mL/2g), bentonite could not close the gaps between the fibers in the bundle and thus, the flow was preferentially occurred through the bundles. Therefore, high hydraulic conductivity was obtained for M_b3 with 15 mM $CaCl_2$. In contrast, with the increase in the MPUA, the hydraulic conductivities were as low as 2.0×10^{-11} m/s within 7 PVF (~170 days) for M_b4 and 9 PVF (~280 days) for M_b5. Then, the hydraulic conductivity of M_b4 and M_b5 increased until 12 PVF (174 days) and 20 PVF (286 days), respectively. Finally, the hydraulic conductivity of GCLs increased up to 2.8×10^{-9} m/s for M_b4 and 1.5×10^{-8} m/s for M_b5.

Figure 3.3b and Figure 3.3c shows the pH and EC values of influent and effluents. Independent of MPUA, the pH of GCLs slightly decreased from 9.4 to 8.0 (Figure 3.3b). Such decrease in pH values has been also reported in literature for the GCLs. The time-dependent dissolution of carbon dioxide (CO_2) from the atmosphere into the permeant solution possibly caused this decrement in pH values (Lee and Schalkelford, 2005). The EC values of effluents have a similar tendency with the Na-GCLs permeated with 6.5 mM $CaCl_2$ solution (Figure 3.2c). From the beginning of the tests, the EC values of GCLs were close to the EC of influent solution. Rapid flow of permeating liquid across M_b3 restricted the reaction time between M_b3 and permeant. Thus, the effluent showed similar characteristics as with influent in terms of EC. In contrast, the EC of M_b4 and M_b5, which have low hydraulic conductivities, was

initially high and decreased until 10 PVFs. Then, EC of the effluent reached the EC of influent. As previously mentioned, the gradual decrease in the EC values can be attributed to continuing cation exchange process during permeation.

Na^+ and Ca^{2+} concentrations detected in the influent and effluent are shown in Figure 3.3d and Figure 3.3e, respectively. The effluent cation concentrations for M_b3 permeated with 15 mM $CaCl_2$ were not measured due to the high hydraulic conductivity of GCL. Nevertheless, the Na^+ concentration decreased (Figure 3.3d) whereas Ca^{2+} concentration increased (Figure 3.3d-e) within 15 PVF for both M_b4 and M_b5. Although the general trend was the same for both GCLs, Ca^{2+} concentrations of the effluent of M_b4 was slightly lower than that of M_b5, but still close to influent concentration (600 mg/L) at the end of the tests. Conversely, Na^+ concentration of the effluent of M_b4 was greater than that of M_b5 (400 vs. 275 mg/L). Based on these analyses, the chemical equilibrium is said to be mostly established for M_b5 and partially established for M_b4. The exchangeable mole fractions of bentonites were determined in terms of Na^+ and Ca^{2+} (i.e. X_{Na} and X_{Ca}). Cation mole fractions were calculated by dividing the concentration of the cation (i.e. Na^+ or Ca^{2+}) to the total concentration of the exchangeable major cations (i.e. Na^+, K^+, Ca^{2+} and Mg^{2+}).

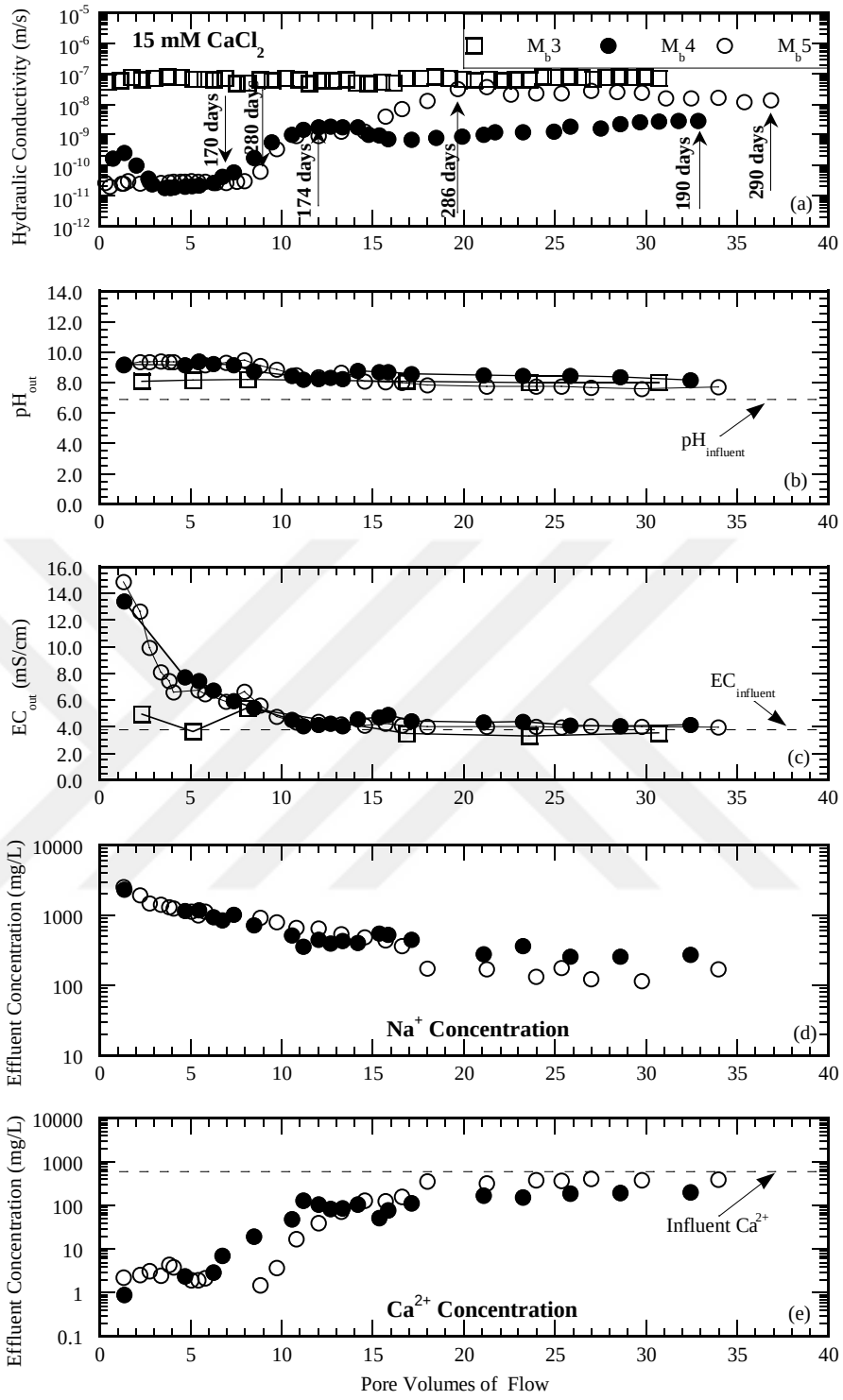

Figure 3.3 a) Hydraulic conductivity behaviors of Na-GCL with M_b3, M_b4 and M_b5 to 15 mM $CaCl_2$ solution, and b) pH, c) electrical conductivity (EC), d) sodium (Na^+) and e) calcium (Ca^{2+}) concentrations of influent and effluent

The change in X_{Na} and X_{Ca} of Na-GCLs were evaluated as a function of MPUA in Figure 3.4a. The mole fractions of virgin (i.e. brand new) GCL was also plotted in Figure 3.4a. The X_{Na} and X_{Ca} of virgin Na-GCL was 0.85 and 0.10, respectively (Figure 3.4a). However, X_{Na} decreased to 0.08 and X_{Ca} increased to 0.82 as the MPUA of GCL increased to 5.0 kg/m^2 (M_b5), indicating cation exchange was less pronounced for M_b3 and more pronounced for M_b5. The reason for this reduction is possibly due to the permeation durations applied on GCLs during the hydraulic conductivity tests.

To show the influence of permeation durations on the cation exchange of Na-GCLs, X_{Ca} of each GCL was divided to their X_{Na} and drawn as a function of permeation duration as shown in Figure 3.4b. The total permeation duration applied for M_b3 was less than one-day because of high hydraulic conductivity measured for this GCL. Since flow mainly occurred through bundle of fibers (Figure 3.5), bentonite reacted limitedly with the permeant and thus, X_{Ca}/X_{Na} was obtained 1.1 for this GCL (Figure 3.4b). This finding also supports the EC measurements of M_b3 (Figure 3.3c). The permeation duration applied on M_b4 and M_b5 was 190 and 290 days which corresponds to X_{Ca}/X_{Na} of 4.8 and 10.7, respectively (Figure 3.4b). The longer permeation duration resulted in a greater X_{Ca}/X_{Na} for M_b5, indicating that the cation exchange is almost complete for this GCL. This finding is also consistent with the effluent concentrations obtained for M_b5 (Figure 3.3d-e) where the Ca^{2+} concentrations were greater and Na^+ concentrations was lower than those of M_b4. The incomplete cation exchange reaction of M_b4 may be the reason why the final hydraulic conductivity of M_b4 was 5.4 times lower than that of M_b5 (2.8×10^{-9} vs. 1.5×10^{-8} m/s). Based on above findings, it can be seen that MPUA as well as permeation duration seem to be important factors while interpreting the hydraulic conductivity and Ca^{2+} breakthrough curves of GCLs.

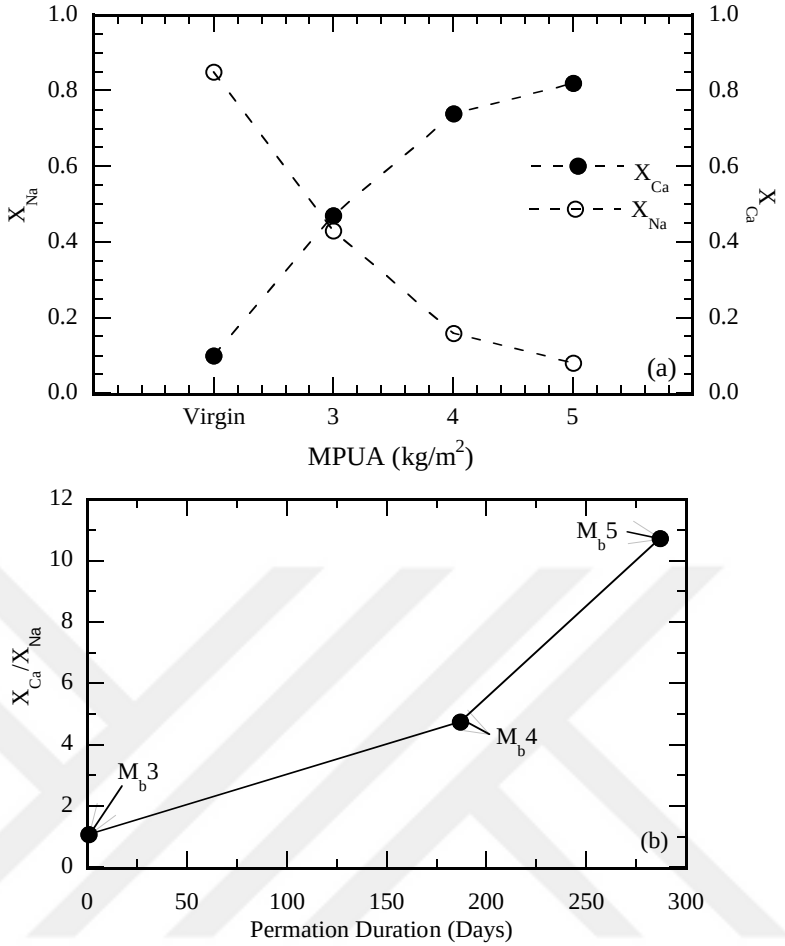

Figure 3.4 Change in the exchangeable cations mole fractions of Na-GCLs as a function of: a) mass per unit area and b) permeation duration

Figure 3.5 General view of M_b3 after permeating with 15 mM $CaCl_2$ solution and dyed regions showing preferential flow paths after dye tests

3.2.5 Hydraulic Conductivity of Na-GCLs to 30 mM $CaCl_2$ Solutions

The hydraulic conductivity of Na-GCLs permeated with 30 mM $CaCl_2$ solutions is shown in Figure 3.6. Since most of the samples pose greater hydraulic conductivity, Na^+ and Ca^{2+} concentrations in the influent and effluent was not analyzed. In contrast, pH and EC were measured, but not presented herein. Note that the measurements are consistent with the hydraulic conductivities.

The initial results of M_b3 and M_b5 (Test 1) were previously reported in Polat et al. (2021) in which the final hydraulic conductivity was 1.3×10^{-7} and 8.3×10^{-9} m/s, respectively. Different from Polat et al. (2021), dye tests were conducted on those GCLs to determine the preferential flow paths across the GCLs. Pink regions in Figure 3.7 demonstrate the flow paths. Although dyed region on M_b5 is very pronounced with respect to that on M_b3, the final hydraulic conductivity of M_b5 was 16 times lower than that of M_b3 (Figure 3.7a-b). When looked closely to M_b5, it was observed that the diameter of bundles on M_b5 was extremely larger than that on M_b3 (Figure 3.7c). However, having greater MPUA led to have lower hydraulic conductivity for M_b5 than for M_b3 (Figure 3.6).

To evaluate the influence of MPUA and bundle of fibers on the hydraulic conductivity, a replicate test was conducted on M_b5. Among M_b5 samples, a visual inspection was made to detect the availability of less bundle of fibers. Then, a candidate M_b5 was selected and tested (Test 2 in Figure 3.6). Indeed, the initial hydraulic conductivity of Test 2 of M_b5 was several orders of magnitude lower than that of Test 1 of M_b5, indicating the effect of bundle of fibers on the hydraulic conductivity during the initial stage of permeation. However, when permeation progressed, the thickness of diffuse double layer surrounding the bentonite compressed as a result of cation exchange and the pressure exerted on the bundles by the swollen bentonite partially released. Hence, preferential flow paths occurred through bundles, resulting in an increase in the hydraulic conductivity of M_b5 (Test 2). Thus, the hydraulic conductivity difference between both tests decreased from several orders of magnitude to a factor of two throughout the test durations.

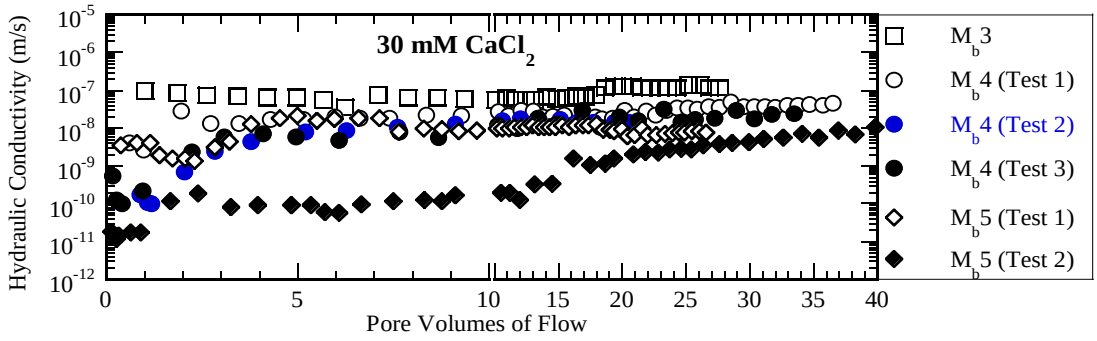

Figure 3.6 Hydraulic conductivity of Na-GCL with M_b3, M_b4 and M_b5 permeated with 30 mM $CaCl_2$ solution

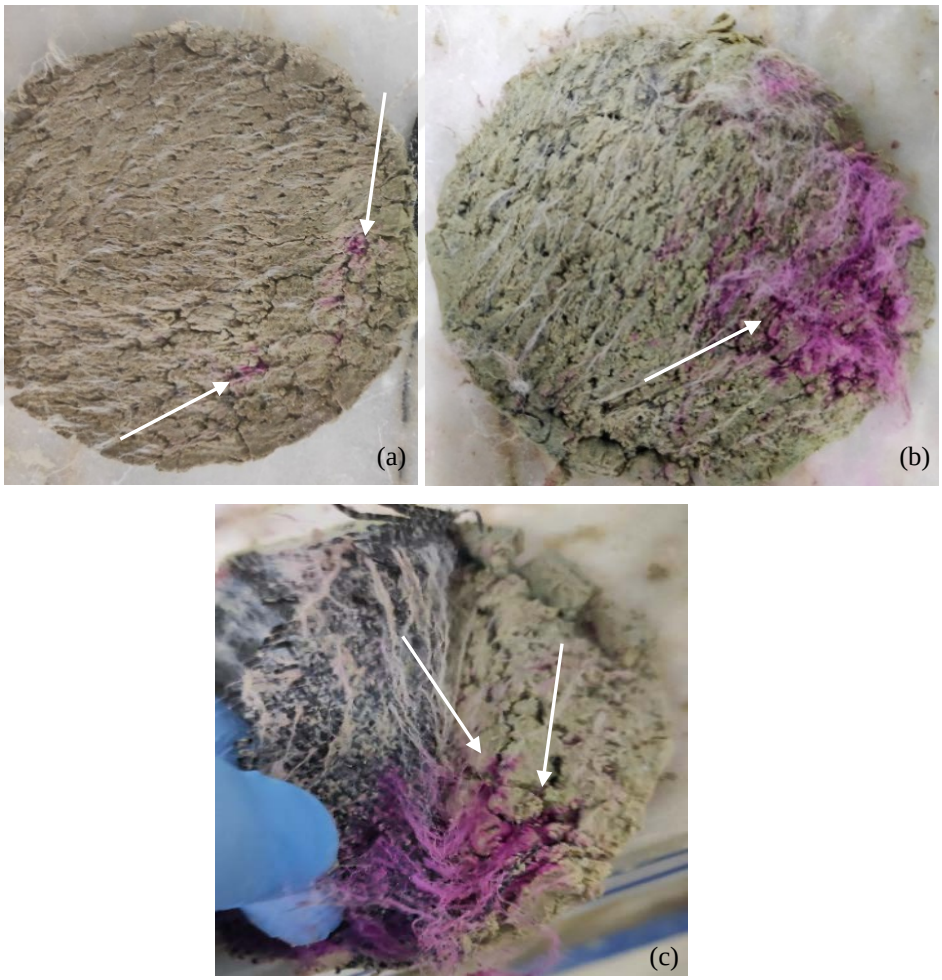

Figure 3.7 General view of bentonites after permeating with 30 mM $CaCl_2$ solution and dyed regions showing preferential flow paths after dye tests: a) M_b3, b) M_b5 (Test 1) and c) close view of bundles on M_b5 (Test 1)

Three hydraulic conductivity tests were conducted on M_b4 (Figure 3.6). The hydraulic conductivity of M_b4 samples were as low as 1.0×10^{-10} m/s during the initial stage of permeation (≤ 1 PVF). Except Test 1 of M_b5, the initial hydraulic conductivities for three tests of M_b4 were in between characteristics of M_b3 and Test 2 of M_b5 (Figure 3.6). When permeation progressed, the pressure acting on the bundles decreases as a result of suppression of thickness diffuse double layer surrounding the bentonite particles because of cation exchange. Hence, the bundle of fibers started to play an important role on transmitting the solution along the micro channel appeared between the fibers.

To examine the influence of MPUA on the hydraulic conductivity of Na-GCLs, the initial and final hydraulic conductivities were plotted as a function of MPUA and shown in Figure 3.8. Note that initial hydraulic conductivity refers to the hydraulic conductivity of GCL at 1PVF. The initial and final hydraulic conductivity of M_b3 is very close to each other, indicating the effectiveness of bundle of fibers from the beginning of the test (Figure 3.8). Since the amount of bentonite is less in M_b3, bentonite swells horizontally when interact with permeating liquid. However, the swelling ability of bentonite in 30 mM $CaCl_2$ solution is limited (Figure 3.1). Thus, the swelling potential of bentonite is enough to close the inter aggregate pores, but it is not fully sufficient to close the channels between the bundle of fibers (Figure 3.5 and Figure 3.7a). Not only M_b4, but also replicates of M_b5 varies within each other (Figure 3.8). However, the initial hydraulic conductivities were remarkably lower than the hydraulic conductivity of M_b3. That is, increasing the bentonite amount in GCL resulted in a reduction in the initial hydraulic conductivities. With the release of pressure exerted on the bundle of fibers as a result of cation exchange, the final hydraulic conductivity of M_b4 and M_b5 increased dramatically (Figure 3.8). However, the final hydraulic conductivity of M_b5 was still lower than that of M_b4 and M_b3.

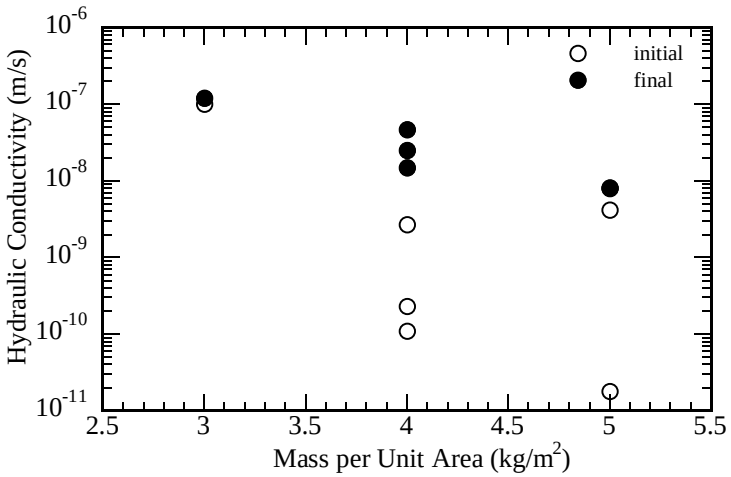

Figure 3.8 Initial and final hydraulic conductivity of Na-GCLs as a function of mass per unit area

3.2.6 Coupled Influence of MPUA and $CaCl_2$ Solution on the Final Hydraulic Conductivity of Na-GCL

The influence of MPUA and the concentration of $CaCl_2$ solutions on the final hydraulic conductivity of Na-GCLs is shown in Figure 3.9. In the case of the hydraulic conductivity to 30 mM $CaCl_2$ solution, the average of three tests for M_b4 and two tests for M_b5 was plotted on Figure 3.9 Decrease in the MPUA and increase in the $CaCl_2$ solution mostly resulted in an increase in the final hydraulic conductivity of GCLs (Figure 3.8). Figure 3.9 also shows that even at low concentration level (i.e. 6.5 mM $CaCl_2$ solution), the hydraulic conductivity of M_b3 was greater than 1.0×10^{-9} m/s which is the maximum hydraulic conductivity suggested for the barriers. At any concentration level, the hydraulic conductivity of GCL decreased about one order of magnitude as the MPUA increased to 5.0 kg/m^2. However, the hydraulic conductivity of M_b4 and M_b5 was still greater than 1.0×10^{-9} m/s when the concentration was increased to 15 mM and 30 mM, indicating insufficient barrier performance achieved even at 5.0 kg/m^2 MPUA.

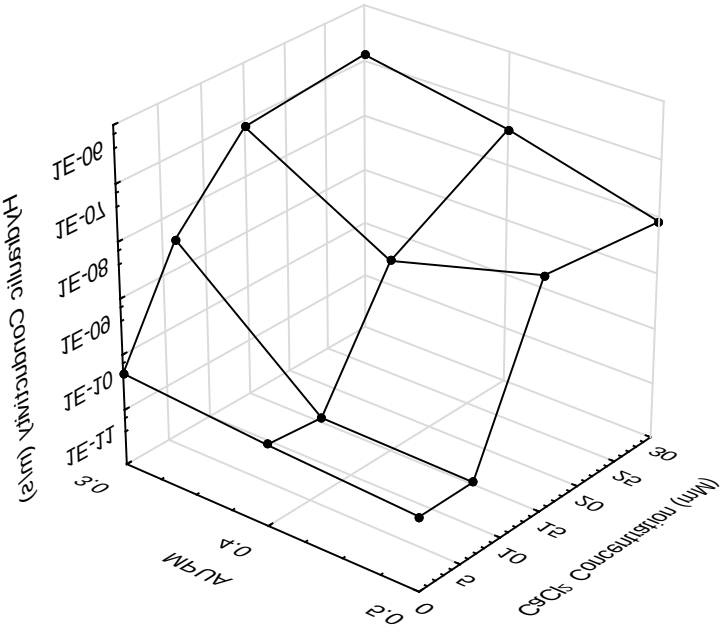

Figure 3.9 Influence of MPUA and concentration of $CaCl_2$ solution on the Na- GCL final hydraulic conductivity

3.3 Influence of MPUA on the barrier performance of P-GCLs

3.3.1 Swell index

The swell index of P-Bentonite is shown in Figure 3.10 as a function of $CaCl_2$ concentration. To make comparison, SI of P-Bentonite was drawn together with that of Na-Bentonite. The SI was determined 23.5 mL/2g in DIW, whereas it was 14.0, 11.0, and 9.5 mL/2g in 15, 30, and 50 mM $CaCl_2$ solutions, respectively. Similar to Na-Bentonite, the swell index of P-Bentonite decreased as the concentration of $CaCl_2$ increased. However, the SI of P-Bentonite is more than SI of Na-Bentonite at any concentration level. The difference is high in DIW (23 vs. 21.5 mL/2g) and less in 30 mM $CaCl_2$ solution (11.0 vs. 10.5 mL/2g). Since the thickness of adsorbed water layer surrounding the bentonite particles are compressed in salt solutions, the SI decreased when $CaCl_2$ concentration in the solution was increased.

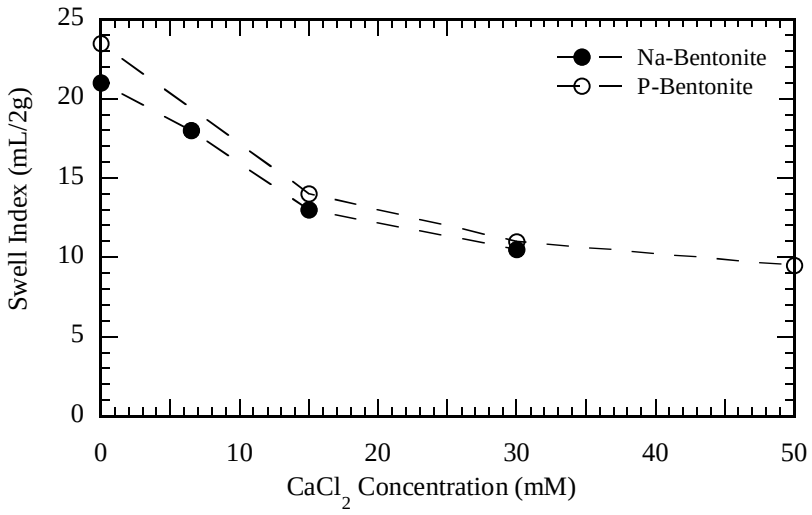

Figure 3.10 Swell indices of Na-Bentonite and P-Bentonite in DIW and $CaCl_2$ solutions

3.3.2 Hydraulic conductivity of P-GCLs

The hydraulic conductivity tests were performed on P-GCLs with MPUA of 3.0,4.0 and 5.0 kg/m^2. The summary of hydraulic conductivity tests is presented in Table 3.2. Regardless of MPUA, the hydraulic conductivity of P-GCL to DIW was approximately the same (average of 3.1×10^{-11} m/s). The hydraulic conductivity of P-GCL to water is similar to hydraulic conductivity of Na-GCL to DIW (average of 3.2×10^{-11} m/s).

Table 3.2 The Final Hydraulic Conductivities of P-GCLs to DIW and $CaCl_2$ Solutions.

Test Number	Measured MPUA (kg/m^2)	Denotation of GCLs	Permeant	Duration (days)	PVF	Hydraulic Conductivity (m/s)
1	3.02	M_b3	DIW	142	6.4	3.4×10^{-11}
2	3.10	M_b3	15 mM $CaCl_2$	39	33	3.5×10^{-9}
3	3.21	M_b3	30 mM $CaCl_2$	19	40	1.9×10^{-7}
4	3.04	M_b3	50 mM $CaCl_2$	0.8	40	5.0×10^{-8}
5	3.95	M_b4	DIW	186	5.1	2.7×10^{-11}
6	4.12	M_b4	15 mM $CaCl_2$	199	27	7.9×10^{-9}
7	4.01	M_b4	30 mM $CaCl_2$	157	46	6.2×10^{-8}

Table 3.2 Continues

8	4.04	M_b4	50 mM $CaCl_2$	40	42	1.7×10^{-8}
9	4.80	M_b5	DIW	175	5.3	3.1×10^{-11}
10	5.00	M_b5	15 mM $CaCl_2$	239	41	1.5×10^{-8}
11	4.92	M_b5	30 mM $CaCl_2$	137	43	1.5×10^{-8}
12	5.16	M_b5	50 mM $CaCl_2$	52	38	1.4×10^{-8}

3.3.3 Hydraulic Conductivity of P-GCLs to 15 mM $CaCl_2$ Solutions

The hydraulic conductivity behavior of P-GCLs to 15 mM $CaCl_2$ solutions is shown in Figure 3.11a as a function of PVF. The hydraulic conductivity of M_b3 was rather high (i.e. 6.0×10^{-10} m/s) at the beginning of the test and then decreased to 5.7×10^{-11} m/s. This decrease can be attributed to the swelling of polymerized bentonite in 15 mM $CaCl_2$ over time. After 4.0 PVF, the hydraulic conductivity rapidly increased and reached ~3.0×10^{-9} m/s until the end of the test. Figure 3.11d-e clearly shows that the sudden increase in hydraulic conductivity of M_b3 is because of the cation exchange. Note that the hydraulic conductivity of Na-GCL with M_b3 was high throughout the test duration and was 7.6×10^{-8} m/s. Measuring lower hydraulic conductivity for Mb3 of P-GCL can be attributed to the polymer loaded on bentonite. On the other hand, the initial hydraulic conductivity of M_b4 and M_b5 was 5.9×10^{-11} and 1.8×10^{-11} m/s, respectively. Although there was a slight decrease in hydraulic conductivity for M_b4, the hydraulic conductivities of M_b4 and M_b5 started to increase after 5 PVFs. M_b4 and M_b5 had similar hydraulic conductivities between 5.0 and 8.0 PVF. However, the hydraulic conductivity of M_b4 increased rapidly after 8.0 PVF, while the hydraulic conductivity of M_b5 increased gradually. That is, while the hydraulic conductivity of M_b4 exceeded above the barrier limit (>1.0×10^{-9} m/s) after 8.0 PVF, the hydraulic conductivity of M_b5 exceeded after 15 PVF. This may be due to the fact that the amount of bentonite in M_b5 is more than M_b4. The hydraulic behavior of Mb4 and Mb5 of P-GCL resembles to that of Na-GCL. However, hydraulic conductivity increased at an earlier PVF for Na-GCL than for P-GCL (7.0 vs 8.0 PVF for M_b4 and

9.0 vs. 15 PVF for M_b5). This also shows how polymer loading delay the hydraulic breakthrough in GCLs.

The pH and EC values of effluents for P-GCLs are shown in Figure 3.11b and Figure 3.11c. At the start of the test, the pH values for all samples were around ~9.5. Then, all slightly decreased until 10 PVF. The final pH of M_b3, M_b4, and M_b5 remained 8.0±0.3 until the end of the tests (Figure 3.11b). Depending on the MPUA, EC values were initially between 15 and 22 mS/cm and decreased over time. After 10 PVF they were almost constant and close to the influent EC value (i.e. 3.8 mS/cm shown with dashed line in Fig. 3.11c).

Figure 3.11d and Figure 3.11e show Na^+ and Ca^{2+} concentrations of effluents of M_b3, M_b4 and M_b5. The effluent concentrations within 5.0 PVF were similar and there were slight variations depending on the MPUA. However, when Ca^{2+} breakthrough at 10 PVF is considered, it can be seen that the concentration obtained for M_b3 was greater than those obtained for M_b4 and M_b5. Similarly, the Ca^{2+} concentration for M_b4 at 10 PVF was greater than that for M_b5. In addition, the breakthrough curves for the Ca^{2+} shown in Fig. 3.11e are very similar to the increases in the hydraulic conductivities of M_b3, M_b4 and M_b5. That is, as the Ca^{2+} concentration increased the hydraulic conductivity of M_b3, M_b4 and M_b5 increased. The cation exchange between Na^+ and Ca^{2+} is the reason governing this tendency.

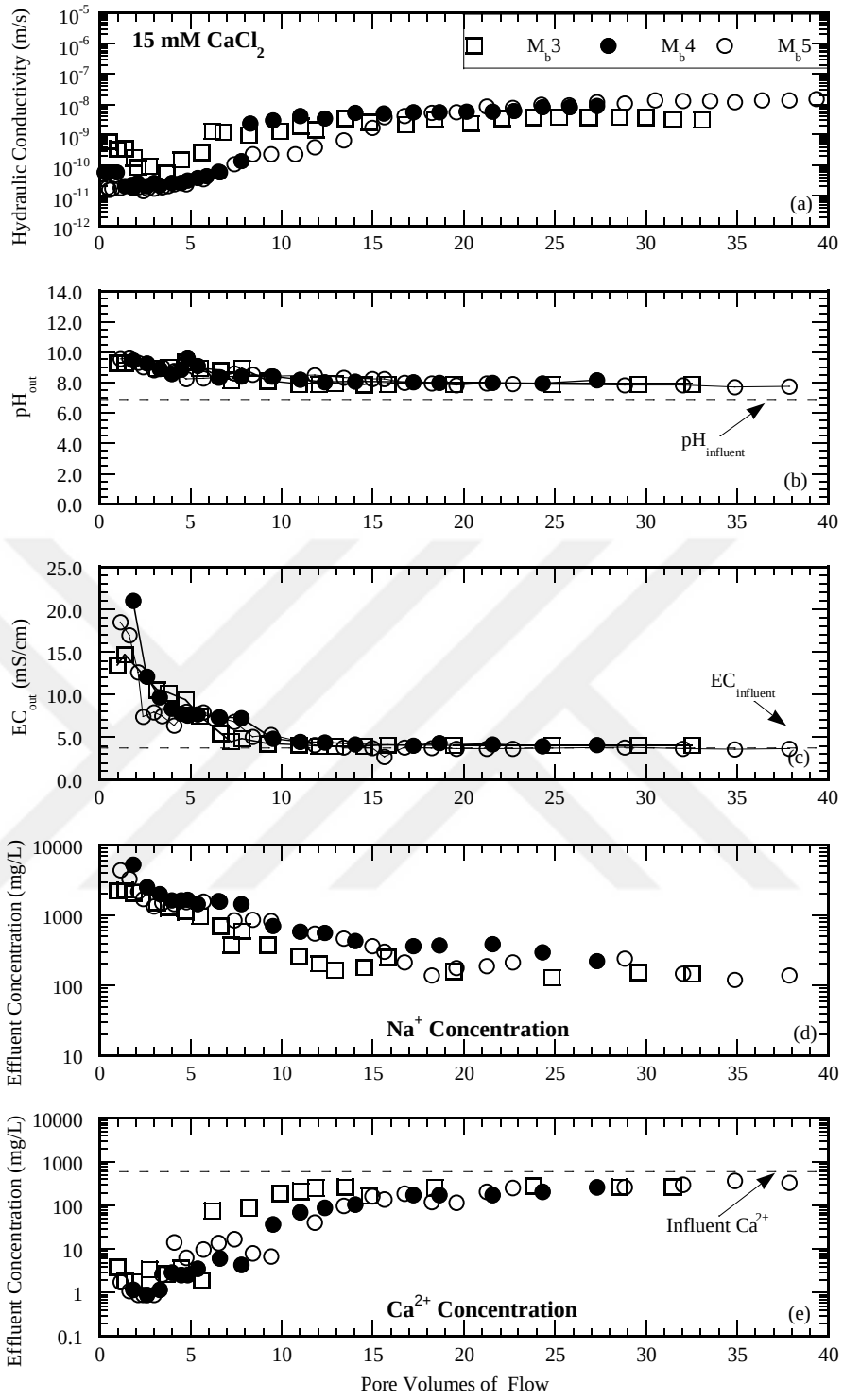

Figure 3.11 a) Hydraulic conductivity behaviors of P-GCLs with M_b3, M_b4 and M_b5 to 15 mM $CaCl_2$ solution, and b) pH, c) electrical conductivity (EC), d) sodium (Na^+), and e) calcium (Ca^{2+}) concentrations of influent and effluent

3.3.4 Hydraulic Conductivity of P-GCLs to 30 mM $CaCl_2$ Solutions

Hydraulic conductivity behaviors of M_b3, M_b4, and M_b5 to 30 mM $CaCl_2$ solutions as well as pH, EC, Na^+, and Ca^{2+} concentrations are shown as a function of PVF and shown in Figure 3.12a-e. As seen in Figure 3.12a, the hydraulic conductivity of M_b3 to 30 mM $CaCl_2$ was around 1.5×10^{-10} m/s from initial to 4.0 PVF. Then the hydraulic conductivity of M_b3 increased and reached 1.7×10^{-7} m/s at the end of the test. Comparing with M_b3 of Na-GCL (Figure 3.6), the initial hydraulic conductivity of P-GCL was significantly low (1.5×10^{-10} vs. 1.0×10^{-7} m/s), but the final hydraulic conductivity is comparable (1.7×10^{-7} vs. 1.2×10^{-7} m/s). The hydraulic conductivity of M_b4 was 3.4×10^{-10} m/s, then slightly decreased until 1.3×10^{-11} m/s. After 3.0 PVF, the hydraulic conductivity started increasing and reached a final value of 6.2×10^{-8} m/s. On the other hand, the hydraulic conductivity of M_b5 was low (~2.0×10^{-11} m/s) until 5.0 PVF from the beginning of the test. Then it increased gradually between 5.0 and 10 PVF and finally, reached to 1.5×10^{-8} m/s thereafter. There was a decreasing trend in the final hydraulic conductivity when MPUA increased from 3.0 to 5.0 kg/m^2. Note that hydraulic conductivity of GCLs increased at an earlier PVF when compared with those permated with 15 mM $CaCl_2$ solution. In addition to this, the hydraulic conductivity of M_b4 and M_b5 of P-GCL was lower than that of M_b4 and M_b5 of Na-GCL in terms of either initial or final hydraulic conductivity.

The pH and EC values of M_b3, M_b4, and M_b5 with 30 mM $CaCl_2$ solutions are shown in Figure 3.12b and Figure 3.12c. Initial pH values for all samples were around 9.2±0.2 then slightly decreased. After 10 PVF, pH values for M_b3, M_b4 and M_b5 almost close to the influent pH value (i.e. 7.6). Initial EC values of M_b3, M_b4, and M_b5 were measured 16.8, 16.6, and 22.1 mS/cm, respectively. Then EC for all samples decreased and reached to 7.0±0.2 which is very close to the EC of influent (i.e. 7.3). Figure 3.12d and Figure 3.12e shows the effluent concentrations of Ca^{2+} and Na^+ for M_b3, M_b4, and M_b5 with 30 mM $CaCl_2$. As seen in Figure 3.12d, Na^+ concentrations were initially high and were 4095, 4262, and 5193 mg/L for M_b3, M_b4, and M_b5, respectively. The greater the relase of Na^+ the greater is the MPUA. Then, Na^+ concentrations decreased for all samples. At the same time, Ca^{2+} concentrations

increased (Figure 3.12e). Regardless of MPUA, Ca^{2+} concentrations reached steady state (or influent Ca^{2+} level) after 15 PVF. Figure 3.12d and Figure 3.12e clearly show that the change in effluent concentrations of Na^{+} and Ca^{2+} is in good aggrement with the hydraulic conductivities shown in Figure 3.12a.

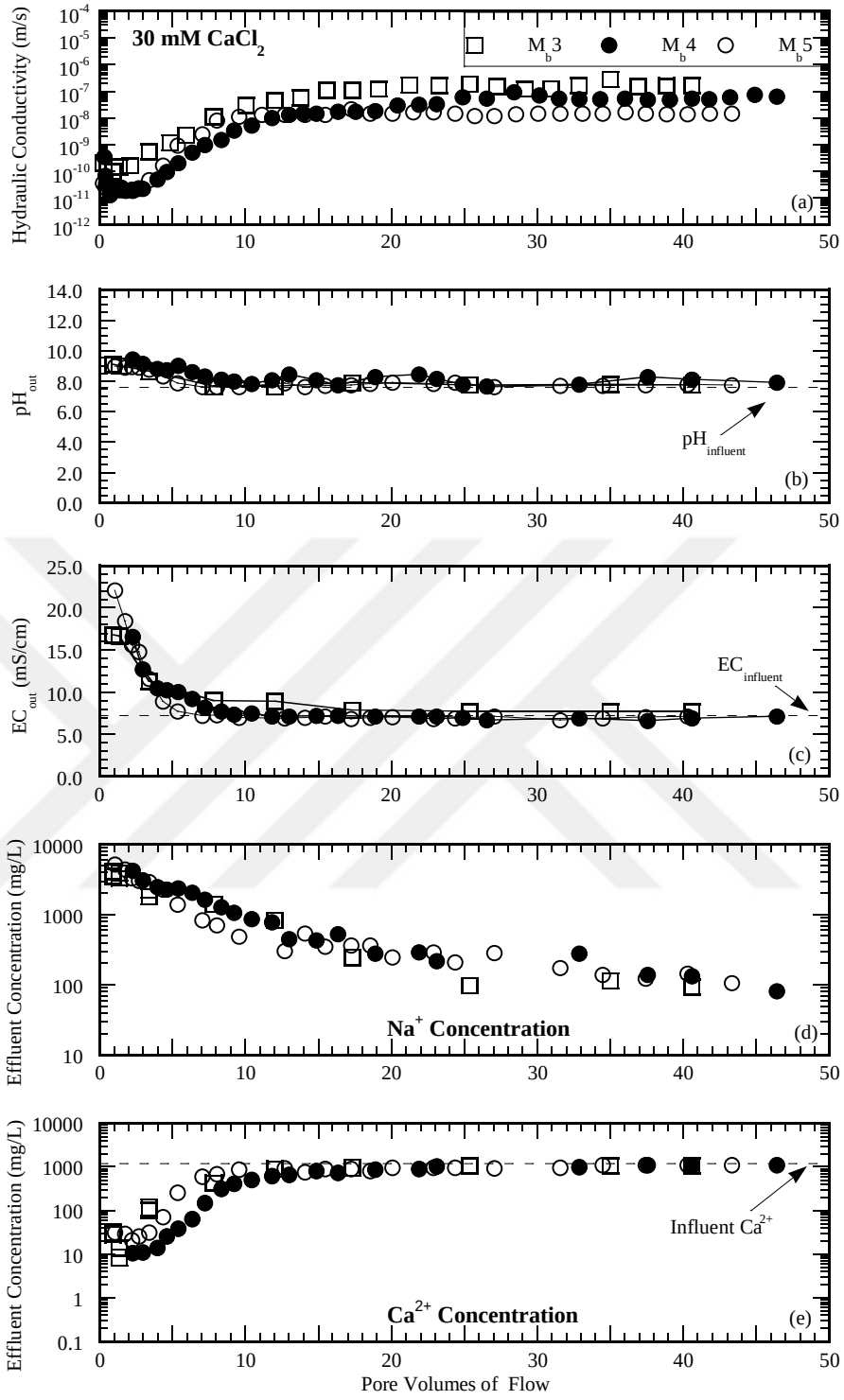

Figure 3.12 a) Hydraulic conductivity behaviors of P-GCLs with M_b3, M_b4 and M_b5 to 30 mM $CaCl_2$ solution, and b) pH, c) electrical conductivity (EC), d) sodium (Na^+), and e) calcium (Ca^{2+}) concentrations of influent and effluent

3.3.5 Hydraulic Conductivity of P-GCLs to 50 mM $CaCl_2$ Solutions

Figure 3.13a-e shows the hydraulic conductivity behaviors of M_b3, M_b4, and M_b5 to 50 mM $CaCl_2$ solutions and pH, EC, Na^+ and Ca^{2+} concentrations measured in the influent and effluents. The hydraulic conductivity of M_b3 was high (5.0×10^{-8} m/s) from the beginning till the end of the test. Although SI was low in 50 mM $CaCl_2$ (Figure 3.10), the hydraulic conductivity behavior of M_b3 was different from M_b4 and M_b5 (Figure 3.13a). This behavior is thought to be related to the less amount of bentonite in M_b3. On the contrary, the hydraulic conductivities of M_b4 and M_b5 were low initially (4.1×10^{-11} and 1.9×10^{-11} m/s, respectively). However, hydraulic conductivity started to increase within a very short time duration.

The pH, EC and effluent cation concentrations for M_b3 permeated with 50 mM $CaCl_2$ were not measured due to high hydraulic conductivity. Figure 3.13b and Figure 3.13c show the pH and EC values of effluents obtained for M_b4 and M_b5. The pH values were around 9.0±0.2 initially and then gradually decreased to the influent pH level (i.e 7.3). Similarly, the initial EC values of M_b4 and M_b5 were 13.8±0.5 mS/cm. Then EC decreased to 11 mS/cm at the end of the tests. The effluent cations of M_b4 and M_b5 are shown in Figure 3.13d and Figure 3.13e. Similar to the previous test results obtained with other $CaCl_2$ concentrations, Na^+ concentrations decreased over time. Note that Ca^{2+} concentrations was initially low however concentrations rapidly increased and approached to the influent Ca^{2+} concentration because of 50 mM $CaCl_2$ solution which is moderately high in concentration.

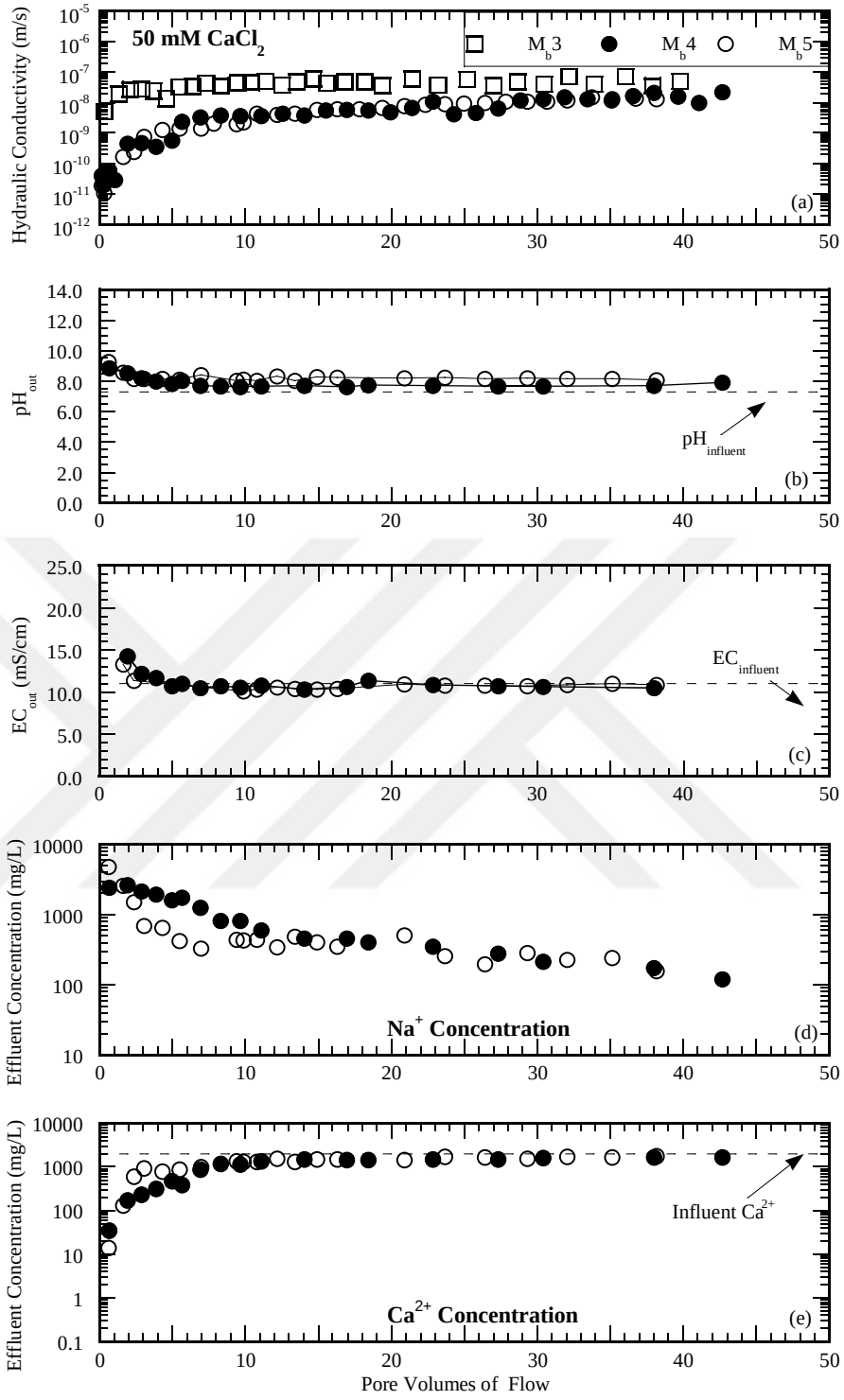

Figure 3.13 a) Hydraulic conductivity behaviors of P-GCLs with M_b3, M_b4 and M_b5 to 50 mM $CaCl_2$ solution, and b) pH, c) electrical conductivity (EC), d) sodium (Na^+), and e) calcium (Ca^{2+}) concentrations of influent and effluent

3.3.6 Influence of MPUA on exchangeable cations of P-GCLs

The change in mole fractions of sodium and calcium (X_{Na} and X_{Ca}) of P-GCLs are shown as a function of MPUA and $CaCl_2$ concentration in Figure 3.14a-b. The X_{Na} and X_{Ca} of virgin P-GCL were determined 0.77 and 0.13, respectively. During hydraulic conductivity tests performed with 15 mM, 30 mM and 50 mM $CaCl_2$ solutions, X_{Na} decreased from 0.77 to the range of 0.05 – 0.23 (Figure 3.14a) and X_{Ca} increased from 0.13 to the range of 0.55 – 0.72 (Figure 3.14b), indicating the cation exchange between GCL and the permeant.

Figure 4.14a also shows that X_{Na} slightly decreased at any concentration level as the MPUA increased. This shows that cation exchange reaction was more when MPUA was 5.0 kg/m^2. In fact, this was expected because the hydraulic conductivity of M_b3 increased at an earlier PVF than that of M_b4 and M_b5. This means less reaction time occurred between M_b3 and $CaCl_2$ solutions. In other words, permeant flowed through the bundles of fibers in M_b3 rapidly and thus, there was not enough time to complete the exchange reaction between Na^+ of bentonite and Ca^{2+} of solution. The above explanation is further supported by the X_{Ca} of the bentonite shown in Figure 4.14b. X_{Ca} of M_b3 was more than that of M_b4 and M_b5, indicating the limited time of exchange reaction.

In the concentration point of view, the least X_{Na} was obtained when the concentration is 30 mM (Figure 4.14a). That is, X_{Na} started to increase when 50 mM was used as the permeant. GCL had time to react with the permeant in terms of cation exchange when concentration was 15 and 30 mM $CaCl_2$ solution. As previously shown in Figure 3.11a and Figure 3.12a, hydraulic conductivity increased within 5-10 PVF and 2-5 PVF in 15 and 30 mM $CaCl_2$ solutions, respectively. However, when 50 mM $CaCl_2$ was used, then hydraulic conductivity increased rapidly which shows very limited time for the cation exchange reaction between GCL and permeant.

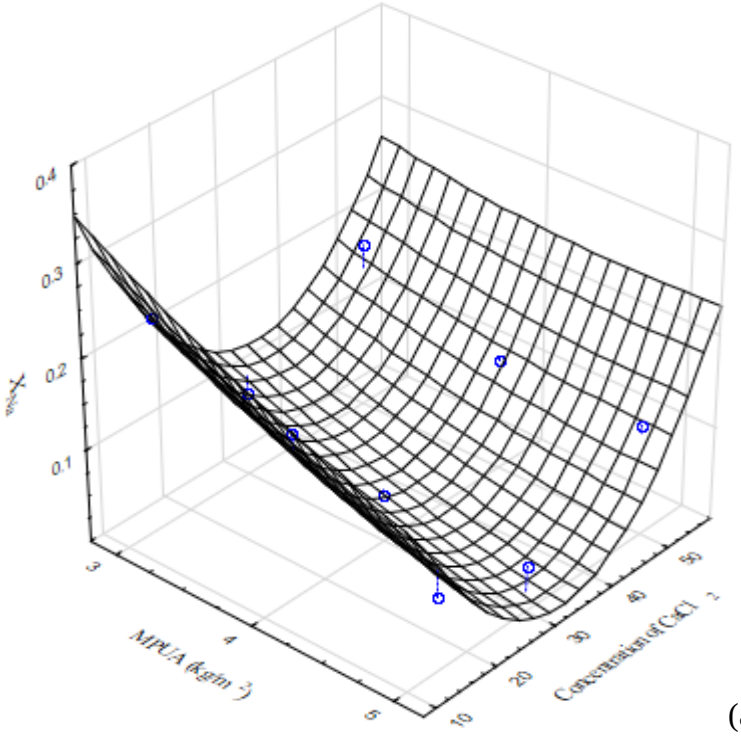

(a)

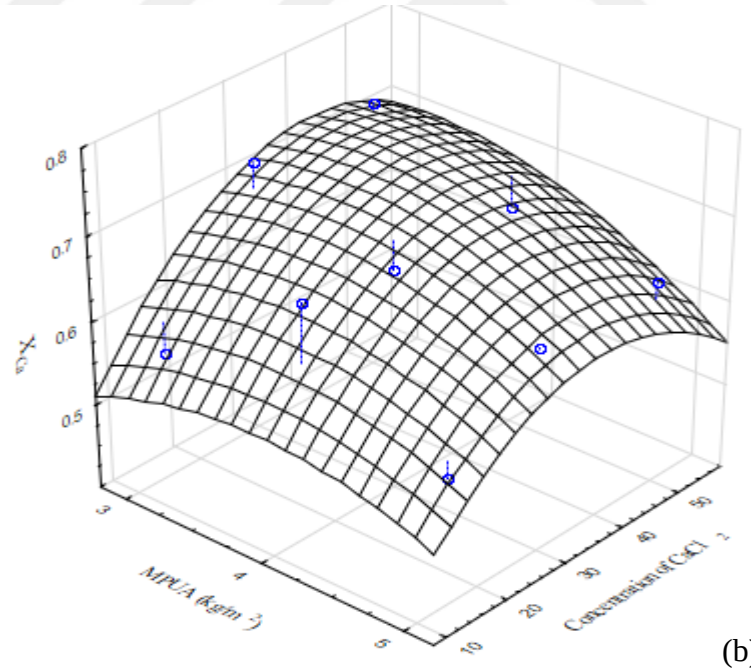

(b)

Figure 3.14 Change in the exchangeable cations mole fractions of P-GCLs as a function of mass per unit area and $CaCl_2$ concentrations: a) X_{Na}, b) X_{Ca}

3.3.6 Coupled Influence of MPUA and $CaCl_2$ Solution on the Final Hydraulic Conductivity of P-GCL

Combined influence of MPUA and $CaCl_2$ solutions on the final hydraulic conductivity of P-GCLs is shown in Figure 3.15. As previously shown in Figure 3.11a, Figure 3.12a, and Figure 3.13a, the initial hydraulic conductivity of Mb3, Mb4, Mb5 to all $CaCl_2$ solutions was low. The hydraulic behaviors of those GCLs showed that hydraulic conductivity inevitably increased as permeation progressed. This is basically because of the existence of bundles of fibers which facilitate the flow across the GCL. As seen in Figure 3.15, the final hydraulic conductivity of GCLs negligibly changed as the MPUA and concentrations of $CaCl_2$ increased. It is important to note that the final hydraulic conductivities of GCLs to $CaCl_2$ solution were above 1.0×10^{-9} m/s which is the limit suggested for the barriers.

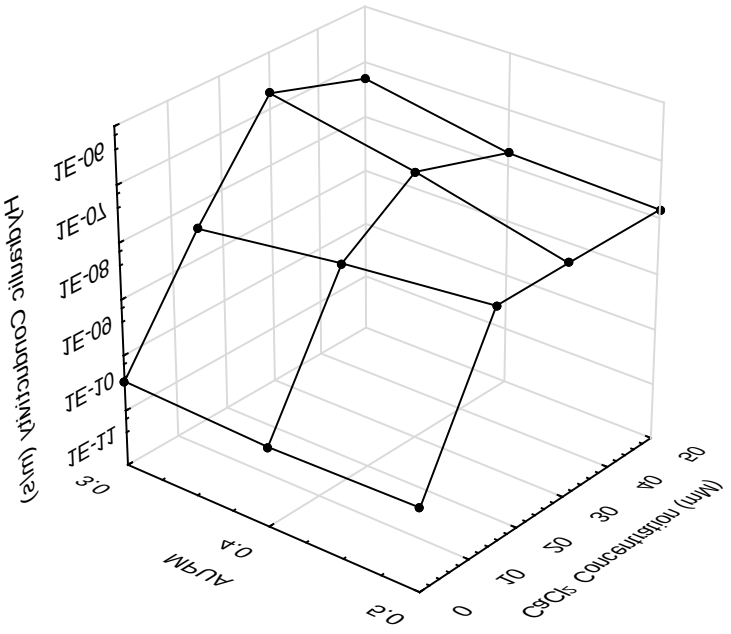

Figure 3.15 Influence of MPUA and concentration of $CaCl_2$ solution on the P-GCL final hydraulic conductivity

3.4 Summary and Conclusions

This study examines the influence of MPUA and the concentration of $CaCl_2$ solution on the barrier performance of GCLs. For this purpose, GCLs with MPUA of 3.0, 4.0, and 5.0 kg/m^2 were conducted to hydraulic conductivity tests with DIW and various concentrations of $CaCl_2$ solutions (6.5 mM, 15 mM, and 30 mM, 50 mM $CaCl_2$). The obtained results are summarized below:

MPUA has negligible influence on the hydraulic conductivity of GCLs when DIW was used as the permeant. This was expected because the hydraulic conductivity of GCLs slightly changed as the MPUA increased.

The influence of MPUA on Na-GCLs was only seen on M_b3 when weak $CaCl_2$ solution (6.5 mM) was used as the permeant. The final hydraulic conductivity of M_b3 was approximately 100 times greater than those of M_b4 and M_b5. Dye test showed that flow preferentially occurred through bundle of fibers available on M_b3.

The hydraulic conductivity behavior of Na-GCLs was separated into two parts as initial and final when an intermediate $CaCl_2$ solution was used (i.e. 15 mM). The hydraulic conductivity of Na-GCL with M_b3 was high along the test duration and was 7.6×10^{-8} m/s. In contrast, the initial hydraulic conductivity of Na-GCLs with M_b4 and M_b5 was as low as 2.0×10^{-11} m/s. However, it started to increase when permeation progressed. The final hydraulic conductivity of M_b4 and M_b5 was 2.8×10^{-9} m/s and 1.5×10^{-8} m/s, respectively, and still lower than that of M_b3. Interestingly, the final hydraulic conductivity of M_b5 was 5 times greater than that of M_b4. However, the breakthrough in the hydraulic conductivity was late for M_b5 than M_b4. That is, hydraulic conductivity started increasing after 170 days of permeation for M_b4 and 280 days of permeation for M_b5, respectively, indicating that the larger MPUA delayed the increase in the hydraulic conductivity of GCLs.

The bound cations of bentonites also gave valuable information about the cation exchange process that took place between permeant and the bentonite. The chemical

analyses showed that Na^+ for Ca^{2+} replacement was almost complete for M_b5. Since breakthrough in the hydraulic conductivity was noticed earlier, the cation replacement was partially fulfilled for M_b4. As a result of cation exchange reaction, the thickness diffuse double layer surrounding the bentonite particles suppressed and therefore, the pressure acting on the bundle of fibers released. Hence, preferential flow paths occurred through the bundles. It may be the reason why the hydraulic conductivity of M_b4 was 5 times greater than that of M_b5. This also shows that the permeation duration is also an important factor controlling not only the cation exchange, but also the hydraulic conductivity.

Similar to 15 mM $CaCl_2$ solution, the initial hydraulic conductivity of Na-GCL with M_b4 and M_b5 was low when $CaCl_2$ solution was increased to 30 mM. However, the breakthrough in the hydraulic conductivity was seen at an earlier PVF for both Na-GCLs when compared to their initial hydraulic conductivities at 15 mM $CaCl_2$ solution. When permeation advanced, the role of bundle of fibers became more pronounced and thus, hydraulic conductivity increased. There was still one order of magnitude difference between the final hydraulic conductivity of M_b3 and M_b5 when tests were ceased. M_b4 and M_b5 did not satisfy the allowable barrier limits suggested by many regulatory agencies (1.0×10^{-9} m/s).

Based on the findings presented herein MPUA and bundle of fibers had significant influence while interpreting the hydraulic conductivity of Na-GCLs, especially when permeated with a solution different than water. Generally, the effects of these factors changed depending on the $CaCl_2$ concentrations and permeation duration. MPUA had a critical role on the hydraulic conductivity behavior when intermediate and strong solutions were used (15 and 30 mM $CaCl_2$, respectively). However, as a result of cation exchange, bundle of fibers started to govern the hydraulic conductivity and thus, hydraulic conductivity increased.

The influence of MPUA and the existence of bundle of fibers on the hydraulic conductivity was evaluated once more on another GCL which includes polymerized bentonite (P-GCL). Again, $CaCl_2$ solutions were used, but at this time instead of 6.5

mM, 50 mM $CaCl_2$ was added to the tests. The initial hydraulic conductivity of P-GCL to 15 mM $CaCl_2$ solution with M_b3 was 10 and 33 times greater than that of M_b4 and M_b5, respectively. Since the bentonite amount of M_b3 is less than the others, it did not sufficient to close the channels available in bundles of fibers. In addition, the hydraulic conductivity of M_b3 and M_b4 increased abruptly while that of M_b5 increased gradually.

When $CaCl_2$ solution was increased to 30 mM, the influence of MPUA on the initial and final hydraulic conductivity of P-GCLs was observed obviously. The average hydraulic conductivities of P-GCL up to 4 PVF were 2.3×10^{-10}, 5.3×10^{-11}, and 2.5×10^{-11} m/s and the final hydraulic conductivities were 1.9×10^{-7}, 6.2×10^{-8}, and 1.5×10^{-8} for M_b3, M_b4, and M_b5, respectively. It is clear to see that there is an increasing trend in the hydraulic conductivity as the MPUA decreased from 5.0 to 3.0 kg/m^2.

Similar conclusion can be drawn in the case of testing with 50 mM $CaCl_2$ solution. That is, the initial hydraulic conductivity of M_b3 was 130 and 240 times greater than that of M_b4 and M_b5, respectively. When final hydraulic conductivity was compared, it was ~3 times greater for Mb3 than for M_b4 and M_b5. In addition, ratio of the initial to final hydraulic conductivity increased as the MPUA decreased. That is, ratio of the initial to final hydraulic conductivity of M_b3 with 50 mM $CaCl_2$ solution was ~10, whereas ~425 and ~660 for M_b4 and M_b5, respectively.

According to the final hydraulic conductivities of P-GCLs, increase in the concentration of $CaCl_2$ caused an increase in the hydraulic conductivity which had been expected. Because similar findings had been initially observed for the Na-GCL.

At the same MPUA and the initial stage of permeation, the hydraulic conductivity of P-GCLs were lower than Na-GCLs. Polymerized bentonite available in P-GCL delayed the increase of hydraulic conductivity by clogging the pores in bundles of fibers. However, regardless of GCL type and MPUA, the hydraulic conductivity increased after a while. This increase was due to washing of polymers from the pores of bundles of fibers. Hence, pores in bundles of fibers started the transmission of flow. Depending on the cation exchange mechanism that took place between Na/P GCL and

permeant, the swell pressure exerted on the bundles reduce and hence, micro channels occur across the GCLs which facilitate flow and increase hydraulic conductivity. Increasing the MPUA delay this behavior for a while but not control the flow individually.

Of course, it would be better if the hydraulic conductivity tests could be conducted with MPUA greater than 5.0 kg/m^2. Thus, it is encouraged to perform hydraulic conductivity tests with greater MPUAs and with different leachates. Simply to make a suggestion for the procedure of testing, many GCL samples should be cut from the roll initially and they should be categorized based on their MPUA. Then, the GCLs with varying MPUAs should be selected and hydraulic conductivity tests should be carried out on these samples. The long term hydraulic conductivity should be determined using site specific solution as the permeant.

CHAPTER FOUR
HYDRAULIC CONDUCTIVITY OF GEOSYNTHETIC CLAY LINERS PRODUCED BY LABORATORY TYPE NEEDLE-PUNCHING APPARATUS

4.1 Background

As previsously mentioned, hydraulic conductivity test is one the most important test method evaluating the barrier performance of GCLs (Özdamar Kul and Ören 2018; Petrov and Rowe 1997). According to studies in the literature, the hydraulic conductivity of GCLs is affected with many factors. Some of these factors were bentonite type, bentonite quality, polymerization of bentonite, bentonite mass per unit area, and the type and concentration of the leachates (D. Kolstad, Benson, and Edil 2004; Lee and Shackelford 2005; Petrov, Rowe, and Quigley 1997). In addition, one of the most important factors is the needle-punching density and bundles of fibers formed during manufacturing process because of needle-punching (Rowe et al. 2017; Salemi et al. 2018). Previous studies conducted on exhumed GCLs showed the significance of the bundle of fibers in GCLs while evaluating the hydraulic conductivity (Rowe et al. 2017; Scalia and Benson 2010, 2011).

Rowe et al. (2017) visualized and digitized the bundle of fiber density and bundle sizes of the GCLs in their studies on exhumed GCLs that were used in the field for 5 and 7 years. They showed that increase in the area covered by bundles and bundle sizes caused an increase in the hydraulic conductivity when GCL was permeated with 10 mM $CaCl_2$ solution.

Salemi et al. (2018) investigated the influence of needle-punching density (15, 30, 45, and 60 /cm^2) on the hydraulic conductivity of GCLs. GCLs was manufactured in the factory and the needle-punching density (NPD) represents the number of needle punches per unit area (cm^2). They conducted hydraulic conductivity tests on GCLs using rigid-wall permeameters and constant-head method. Although deionized water was used as the leachate in the hydraulic conductivity tests, high hydraulic

conductivity values (>10^{-7} m/s) were observed in all samples. As a result of their study, the highest hydraulic conductivity was obtained on the GCL that had the highest NPD.

In the previous chapter, it has been emphasized that the gradual increase in the hydraulic conductivity was attributed to the cation exchange. With the replacement of Na^{+} with Ca^{2+}, the pressure acting on the fibers decrease and therefore, micro-channels occur along the fibers which transmits flow of $CaCl_2$ solution. Thus, the existence of bundles of fibers across the GCL is an important phenomenon that is why the influence of NPD on the hydraulic conductivity of GCL was investigated in the content of this study as well. Therefore, a laboratory type needle-punching apparatus was designed and manufactured to produce artificial GCLs (A-GCLs) at desired NPDs (5, 10, and 15 /cm^2). The hydraulic conductivity tests were conducted in flexible-wall permeameter cells with different concentrations of $CaCl_2$ solutions (15, 30, and 50 mM). Since chemical tests were not performed on effluents of A-GCLs, the comparison of artificial and original GCL was made only in terms of hydraulic conductivity.

4.2 Laboratory Type Needle-Punching Apparatus

Laboratory type GCL needle-punching apparatus was designed in order to produce A-GCLs at the desired NPDs (Figure 4.1a-d). The apparatus consists of a conveyor belt, needle-punching stand, and some mechanical parts. Two L profiles were used to create a 600 mm long and 230 mm wide conveyor frame. Also, a 180 mm wide belt was manufactured. Afterward, various connection holes were drilled on the frame of the conveyor. Bearings were mounted and the conveyor belt system was completed. In order to make the needle-punching movement, the movable arm mechanism was designed and the necessary parts (various gears and chains) were procured and adapted to the system.

The mechanical arm used has the ability to move up and down, thanks to the spring system it contains (Figure 4.1a-d). The movement of the arm helps GCL to move forward on the band while needle punching process was applied. In the designed

system, the downward movement of the arm compresses the spring in the mechanism and hence, enables the punching of the GCL. With the removal of the force applied on the arm, the mechanism moved upward direction (the spring will return to its first position) and GCL progressed on the band. In order to adjust the amount of movement of the GCL on the band (i.e. band step), the vertical movement interval of the apparatus was designed to be changeable. This design allowed apparatus to change the NPD at desired rates while manufacturing.

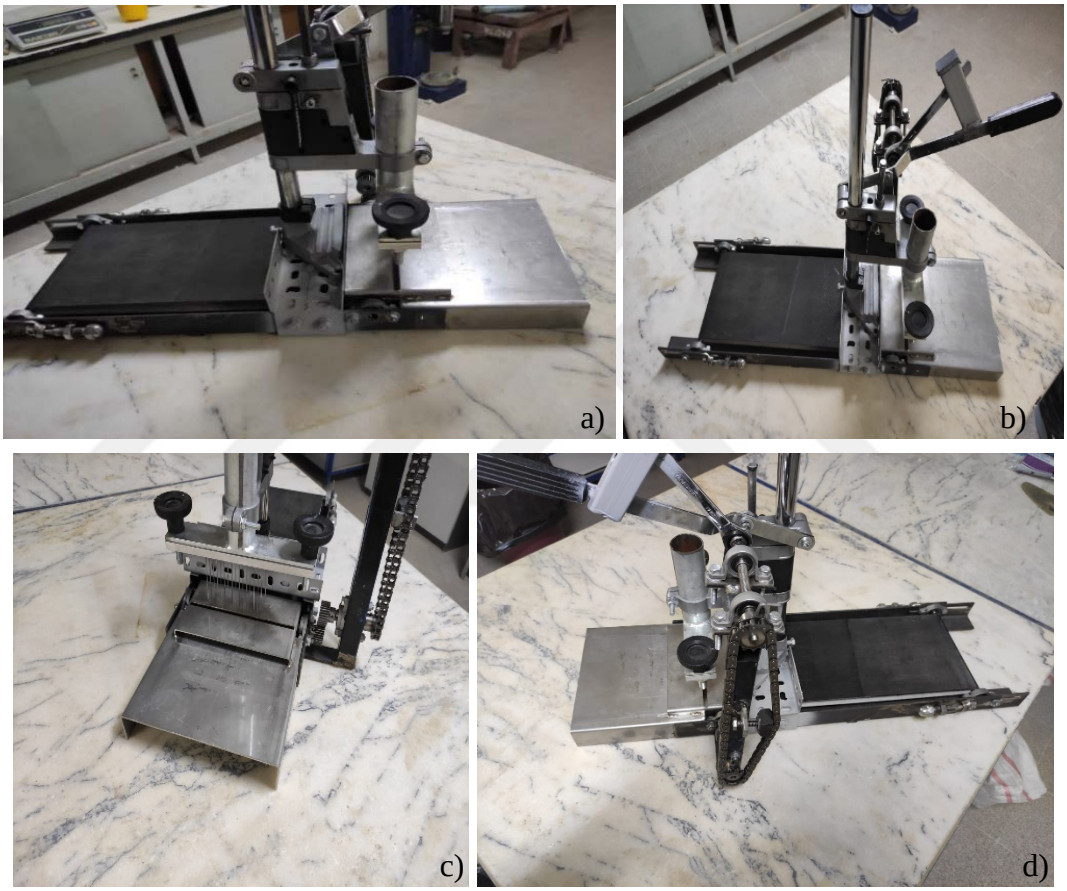

Figure 4.1 Photographs of laboratory type GCL needle-punching apparatus: a) left close view, b) left view, c) front view, and d) right view

The type of needles which will be used for the process of needle-punching of GCLs were also investigated. For this purpose, an interview was made with an international company that produces needles. Based on the suggestion, two needles with backward notches were supplied from the company. After the needles were procured, needle tray

design was carried out. Considering the needle sizes, 2 mm diameter holes were drilled on the steel rigid plate so that the needles could be placed comfortably. This plate is so-called needling table. In order to use different NPDs and needle-punching patterns during production, the holes in the needling table were drilled in 3 rows with 2 mm intervals horizontally and 2.5 mm vertically. The final view of needle-punching table and needles with backward notches are shown in Figure 4.2a and Figure 4.b, respectively.

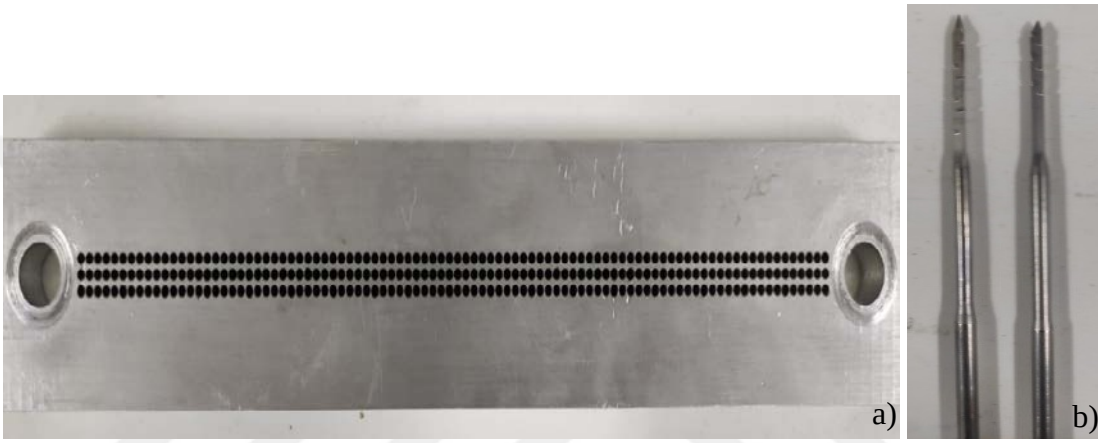

Figure 4.2 Photographs of materials in laboratory type GCL needle-punching apparatus: a) needling table and b) needles with backward notches

4.2 Manufacturing of Artificial GCL

Woven and nonwoven geotextiles of original P-GCL were supplied from the manufacturer for the production of A-GCLs. In addition, polymer bentonite was extruded from P-GCL roll and used in A-GCLs. The roll system used for stretching the textiles during fabrication production was represented by the rectangular frame system in the laboratory (Figure 4.3a). For the manufacturing of A-GCLs, first of all, a woven geotextile was placed on the outer frame (Figure 4.3b), then bentonite was sprinkled (Figure 4.3c), and a nonwoven geotextile was placed on bentonite (Figure 4.3d). After the inner frame was adapted to the system, the tension of the sample was adjusted by tightening the tension screws (Figure 4.3e).

The sample placed in the frame system was then moistened with the help of a sprayer containing DIW, similar to the sprinkling method used in industrial manufacturing. The sample was placed on the conveyor belt and positioned in the needle-punching unit (Figure 4.3f). After the necessary controls were made in terms of manufacturing, the needle-punching process was started mechanically which means applying a force by hand (Figure 4.3g). The mechanical arm was moved up and down in order to perform the needle-punching. The downward movement of the arm provided the needling of the GCL, while the upward movement of the arm moved the conveyor and hence, the sample (Figure 4.3g).

Figure 4.3 Photographs of A-GCLs during manufacturing: a) rectangular production frame, b) woven geotextile placed in the outer frame, c) bentonite placement on woven geotextile, d) non-woven geotextile overlying bentonite, e) placement of inner frame, f) sample ready for the needling, and g) manufacturing of A-GCL

Some of the A-GCLs manufactured using the laboratory type needle-punching equipment are shown in Figure 4.4. Figure 4.4a shows the woven face, whereas Figure 4.4b shows the non-woven face of A-GCL. Figure 4.4c shows other A-GCLs produced with the same manner.

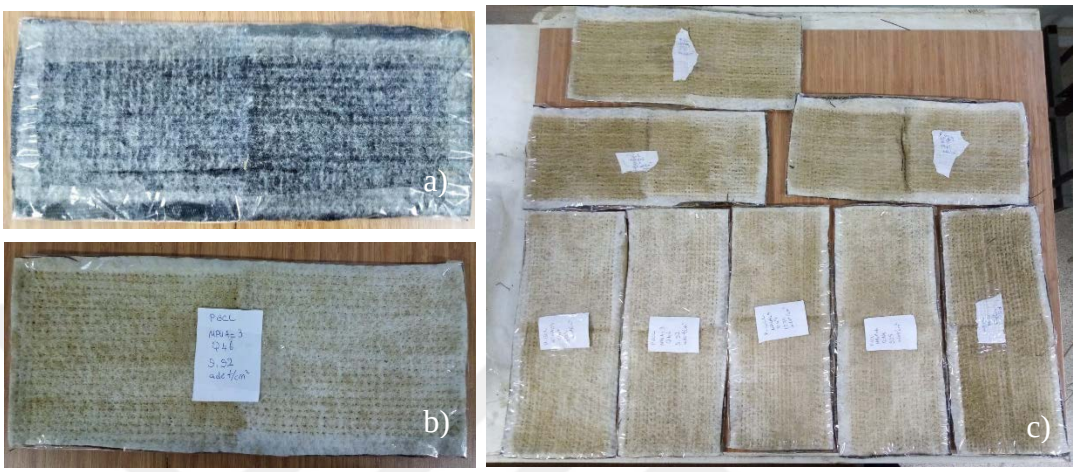

Figure 4.4 Appearance of A-GCLs after production: a) woven face, b) non-woven face, and c) other A-GCLs

Three different NPDs (low, medium, and high) were targeted during the manufacturing of GCLs. The initial step of manufacturing was trial and counting the density of punching. As a result of trial and error process, it was decided to place needles in the first row of plate shown in Figure 4.2. With this configuration, 5 punches per unit area (cm^2), namely 5 NPD, were achieved on the GCL mounted frame system. That is, one round of needle-punching on the GCLs with the maximum needle frequency was equal to 5 /cm^2 NPD. Thus, the minimum bundle of fiber formation was achieved with 5 /cm^2 needle-punching (low density) during GCL manufacturing. To achieve medium density (~10 /cm^2) and high-density (~15 /cm^2), the GCL mounted rectangular frame was passed two and three times, respectively, through the apparatus. The designed apparatus enables up to 15 NPD on GCLs. Further increase in the NPD led to occurrence of holes on the GCLs in which the bentonite started to come out. Once the manufacturing completed, the densities were verified by dividing the needle-punched area by the product of the number of arm descents and the number of needles.

In the scope of the study, hydraulic conductivity tests were conducted on GCLs that have three different bentonite MPUAs and three different NPDs. The MPUA of GCLs were categorized as low (between 2.78-3.68 kg/m^2, M_b~3), medium (between 4.76-6.02 kg/m^2, M_b~5), and high (between 6.81-7.75 kg/m^2, M_b~7). Artificial GCLs for ease of expression throughout the text, will be named depending on the NPD and MPUA. For example, A5L stands for A-artificial, 5- 5/cm^2 NPD and L- low MPUA. In addition to this, P-GCLs will be named henceforth as original L (original P-GCL with low MPUA) and original M (original P-GCL with medium MPUA). Figure 4.5 shows the comparison of A-GCLs and original P-GCL. As seen in Figure 4.5, A15M resembles to the original GCL. Because the white area on the A-GCL increased as the NPD increased. However, the NPD of original P-GCL still seems to be greater than A-GCLs which may be due to more intense needle-punching during manufacturing by machine.

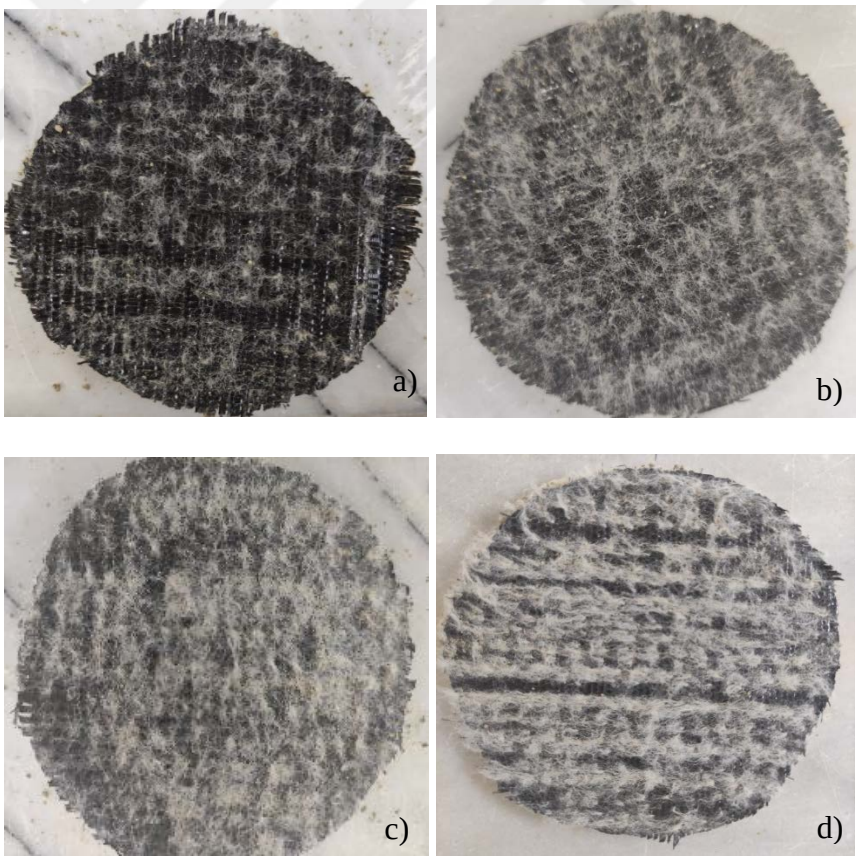

Figure 4.5 Artificial and original GCLs: a) A5M, b) A10M, c) A15M and d) original M

4.3 Hydraulic Conductivity of A-GCLs

Total of 26 hydraulic conductivity tests were conducted on A-GCLs. Tests were performed using 15, 30, and 50 mM $CaCl_2$ solutions. Hydraulic conductivity of original P-GCLs to $CaCl_2$ solutions were taken from Chapter 3 to compare with that of A-GCLs. Hydraulic conductivity of P and A-GCLs is summarized in Table 4.1.

Table 4.1 The Final Hydraulic Conductivities of A-GCLs to $CaCl_2$ Solutions

Test Number	Measured MPUA (kg/m^2)	Denotation of GCLs	Permeant	Duration (days)	PVF	Hydraulic Conductivity (m/s)
1*	2.78	A5L	15 mM $CaCl_2$	45	21	2.1×10^{-9}
2*	3.53	A10L	15 mM $CaCl_2$	53	26	2.4×10^{-9}
3*	3.38	A15L	15 mM $CaCl_2$	73	19	1.0×10^{-8}
4**	3.10	Original L	15 mM $CaCl_2$	39	33	3.5×10^{-9}
5	3.38	A5L	30 mM $CaCl_2$	29	30	1.2×10^{-8}
6*	3.63	A10L	30 mM $CaCl_2$	68	7.8	4.6×10^{-10}
7	3.50	A15L	30 mM $CaCl_2$	28	29	2.0×10^{-8}
8**	3.21	Original L	30 mM $CaCl_2$	19	40	1.9×10^{-7}
9	3.30	A10L	50 mM $CaCl_2$	38	27	8.5×10^{-9}
10*	3.49	A15L	50 mM $CaCl_2$	69	18	1.9×10^{-9}
11**	3.04	Original L	30 mM $CaCl_2$	0.8	40	5.0×10^{-8}
12*	5.57	A5M	15 mM $CaCl_2$	250	6.4	5.8×10^{-11}
13	4.89	A10M	15 mM $CaCl_2$	177	33	1.3×10^{-8}
14*	5.17	A15M	15 mM $CaCl_2$	300	5.7	2.1×10^{-11}
15**	5.00	Original M	15 mM $CaCl_2$	239	41	1.5×10^{-8}
16	5.06	A5M	30 mM $CaCl_2$	120	35	1.6×10^{-8}
17	4.76	A10M	30 mM $CaCl_2$	105	39	4.1×10^{-9}
18	5.33	A15M	30 mM $CaCl_2$	130	31	4.2×10^{-9}
19*	4.92	Original M	30 mM $CaCl_2$	137	43	1.5×10^{-8}

Table 4.1 Continues

20*	5.65	A5M	50 mM $CaCl_2$	167	9	6.1×10^{-10}
21	5.30	A10M	50 mM $CaCl_2$	108	30	7.0×10^{-9}
22*	6.02	A15M	50 mM $CaCl_2$	204	7.1	9.3×10^{-11}
23**	5.16	Original M	50 mM $CaCl_2$	52	38	1.4×10^{-8}
24*	7.23	A5H	15 mM $CaCl_2$	227	3.2	2.9×10^{-11}
25*	7.20	A10H	15 mM $CaCl_2$	254	3.4	5.6×10^{-11}
26*	7.75	A15H	15 mM $CaCl_2$	238	4.8	5.8×10^{-11}
27*	7.04	A5H	30 mM $CaCl_2$	114	1.5	2.6×10^{-11}
28*	7.14	A10H	30 mM $CaCl_2$	217	4.1	7.4×10^{-11}
29*	6.81	A15H	30 mM $CaCl_2$	232	14	1.4×10^{-9}
30*	6.91	A5H	50 mM $CaCl_2$	132	2.0	3.8×10^{-11}
31*	6.77	A10H	50 mM $CaCl_2$	206	3.8	7.7×10^{-11}
32*	6.96	A15H	50 mM $CaCl_2$	223	11	1.5×10^{-9}

* Continues

** Results taken from Chapter 3 in section P-GCLs hydraulic conductivities

4.3.1 Hydraulic Conductivity of A-GCLs to 15 mM $CaCl_2$ Solutions

The hydraulic conductivity behavior of GCLs with low MPUA (M_b~3) is shown in Figure 4.6 when GCLs were permeated with 15 mM $CaCl_2$ solutions. The initial hydraulic conductivity (up to 1 PVF) of the original L GCL was 4.7×10^{-10} m/s. Then, it decreased to 5.7×10^{-11} m/s. After 4 PVF, the hydraulic conductivity of original L increased up to 3.5×10^{-9} m/s. The initial hydraulic conductivity of A5L was 6.6×10^{-9} m/s. Then, it decreased slightly. Following this decrement, the hydraulic conductivity of A5L increased after 4 PVF which was similar to that of original L. On the other hand, the initial hydraulic conductivity of A10L and A15L were low (2.1×10^{-11} and 6.7×10^{-11} m/s, respectively). Then, the hydraulic conductivities started to increase. When compared to the original L, very similar hydraulic behaviors were obtained with

A-GCLs regardless of NPD. Especially, the final hydraulic conductivities were within the range of 2.1×10^{-9} - 1.0×10^{-8} m/s all of which are above the limit suggested for the barriers. Note that, the hydraulic conductivity of A-GCLs have not been terminated.

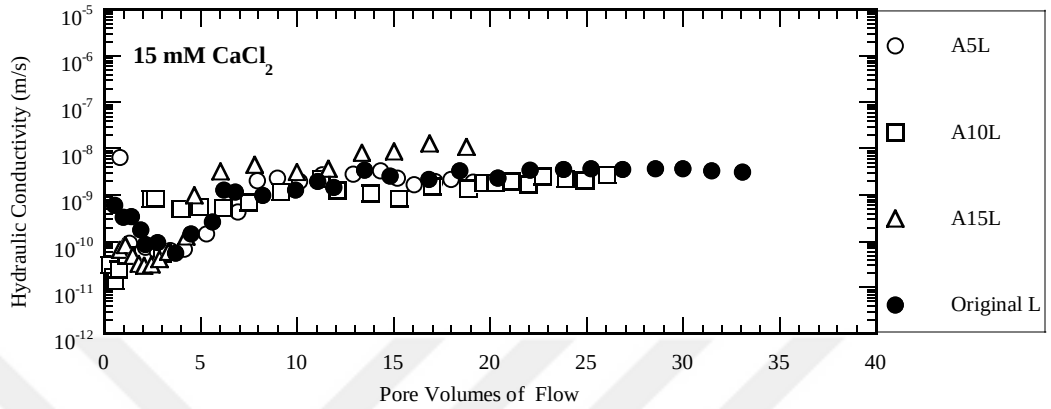

Figure 4.6 Hydraulic conductivity behaviors of GCLs with low MPUA (M_b~3) to 15 mM $CaCl_2$ solution

The hydraulic conductivity behavior of GCLs with medium ($M_{b\sim5}$) MPUA is shown in Figure 4.7. A-GCLs were permeated with 15 mM $CaCl_2$ solution. As can be seen in Figure 4.7, similar behaviors were observed up to approximately 4 PVFs for the original and artificial GCLs where the hydraulic conductivity values were found ~5.0×10^{-11} m/s. However, about 2500 times increase in the hydraulic conductivity of the original M and A10M was observed until the end of tests. A5M and A15M have been still in progress and the permeation time slightly exceeded 5 PVF. Considering the last readings, it can be seen that the hydraulic conductivity values of these samples also tended to increase. On the other hand, the final hydraulic values of the original M and A10M, in which physical stability was achieved in terms of hydraulic conductivity, were measured 1.5×10^{-8} and 1.3×10^{-8} m/s, respectively.

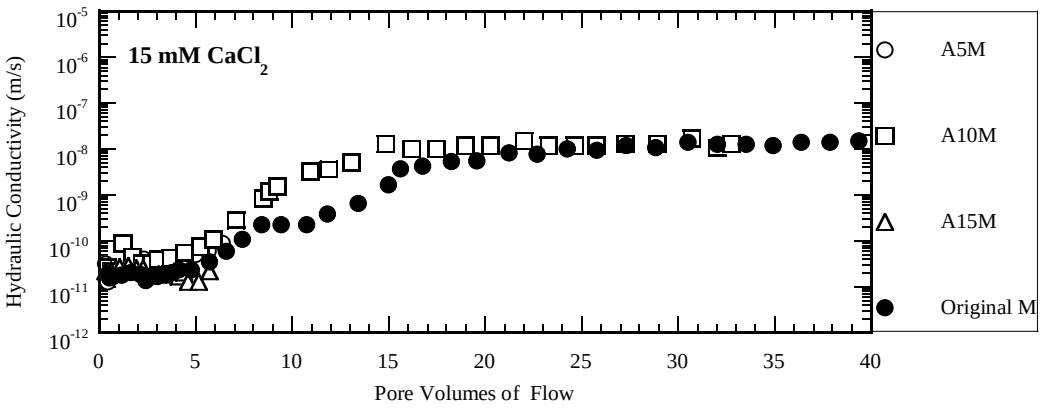

Figure 4.7 Hydraulic conductivity behaviors of GCLs with medium MPUA (M_b~5) to 15 mM $CaCl_2$ solution

The hydraulic conductivity tests on high MPUA (M_b~7) of A-GCLs to 15 mM $CaCl_2$ solutions is shown in Figure 4.8. Only the hydraulic conductivity of A-GCL is plotted in Figure 4.8, since original GCL did not contain high MPUA region on roll. According to Figure 4.8, A5H, A10H, and A15H have similar hydraulic conductivity behaviors and their hydraulic conductivities were approximately 3.0×10^{-11} m/s. Although the hydraulic conductivity of A10H and A15H slightly increased, they are still low ($< 1.0\times10^{-10}$ m/s). These tests have not been terminated yet.

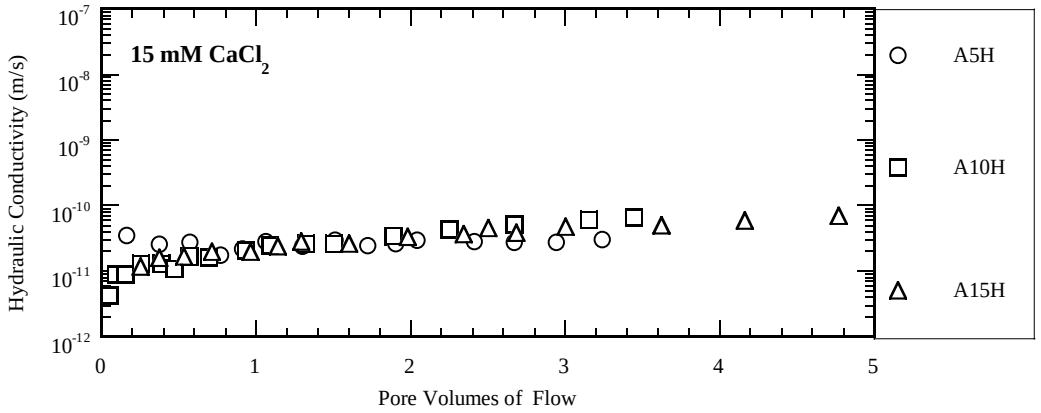

Figure 4.8 Hydraulic conductivity behaviors of GCLs with high MPUA (M_b~7) to 15 mM $CaCl_2$ solution

4.3.2 Hydraulic Conductivity of A-GCLs to 30 mM $CaCl_2$ Solutions

The hydraulic conductivity of M_b~3 to 30 mM $CaCl_2$ is shown in Figure 4.9 as a function of PVF. The initial hydraulic conductivity of A-GCLs were around 5.0×10^{-11} m/s whereas the original L was 1.0×10^{-10} m/s which is two times greater than artificial GCLs. After 3 PVF permeation, the hydraulic conductivities increased for all GCLs. Based on the final hydraulic conductivities, original L was 10 times greater than A5L and A15L. Nevertheless, the final hydraulic conductivities of all these samples were above the barrier limit. On the other hand, the hydraulic conductivity test on A10L is still in progress of which started to increase and the general trend resembles to other GCLs. According to last readings, the hydraulic conductivity of A10L was approximately 4.6×10^{-10} m/s.

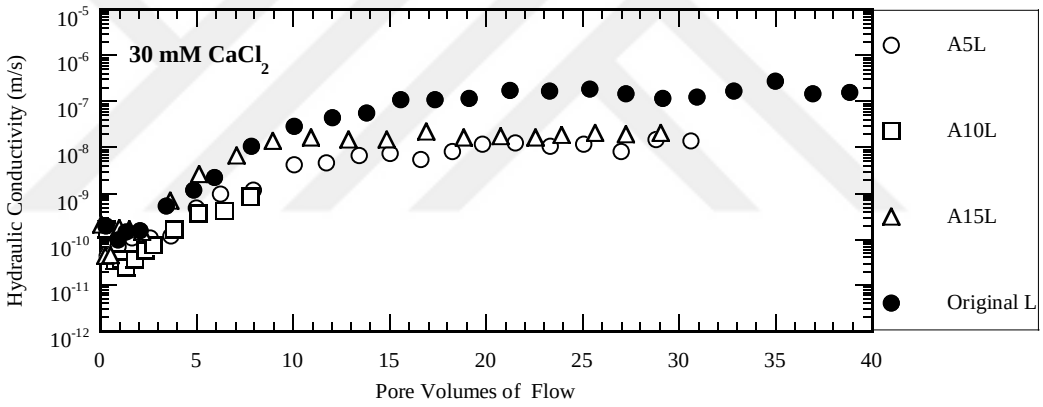

Figure 4.9 Hydraulic conductivity behaviors of GCLs with low MPUA (M_b~3) to 30 mM $CaCl_2$ solution

The hydraulic behavior of M_b~5 of original and A-GCLs permeated with 30 mM $CaCl_2$ solution is shown in Figure 4.10. The hydraulic conductivity trend was very similar to that obtained with 15 mM $CaCl_2$ solution. While the hydraulic conductivities were around ~10^{-11} m/s at the beginning of the tests (up to ~3 PVF) in all GCLs, but they increased over time (~10^{-8} - 10^{-9} m/s). However, with increasing the solution concentration, the hydraulic conductivity of the GCLs started to increase in an earlier PVF. It can be said that this situation is due to the fact that bentonite is exposed to faster cation exchange with the increase in solution concentration (Lee and Shackelford 2005).

The final hydraulic conductivity of the original M was 1.5×10^{-8} m/s, while A5M was measured 1.6×10^{-8} m/s. The difference between two GCLs is comparable. The hydraulic conductivities of A10M and A15M were 4 times lower than that of A5M and original GCL and were 4.1×10^{-9} m/s and 4.2×10^{-9} m/s, respectively. When the results are evaluated together, it can be said that this difference between the hydraulic conductivity values of the original and artificial GCLs is within an acceptable level. However, it is seen that the final hydraulic conductivity values obtained are above the barrier limit ($>10^{-9}$ m/s).

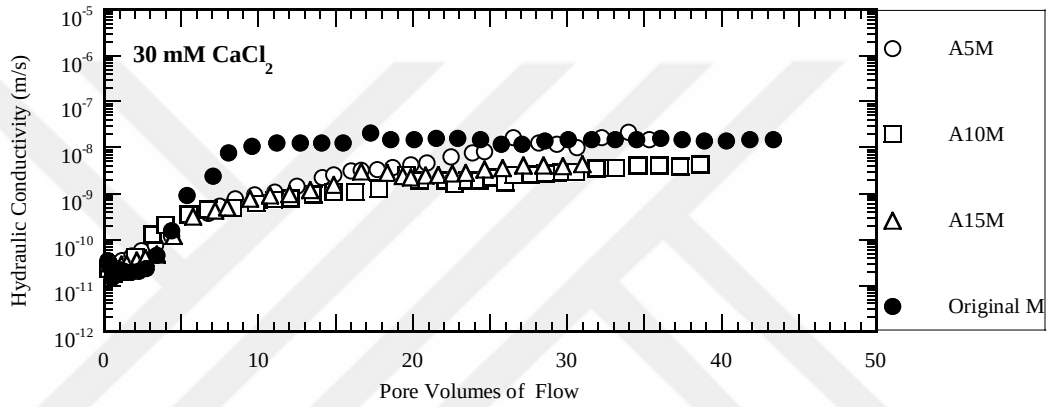

Figure 4.10 Hydraulic conductivity behaviors of GCLs with medium MPUA (M_b~5) to 30 mM $CaCl_2$ solution

The hydraulic conductivity of A-GCLs with high MPUA (M_b~7) permeated with 30 mM $CaCl_2$ is shown in Figure 4.11. The initial hydraulic conductivity of A-GCLs was around ~2.0×10^{-11} m/s. Considering the last reading, the hydraulic conductivity of A5H was still low and A10H slightly increased after 2 PVF and reached 9.9×10^{-11} m/s. On the other hand, the hydraulic conductivity of A15H increased after 4 PVF permeation. The last readings show that the hydraulic conductivity of A15H was 1.4×10^{-9} m/s. None of tests shown in Figure 4.11 has been completed. Thus, the hydraulic conductivity of these samples inevitably change until termination.

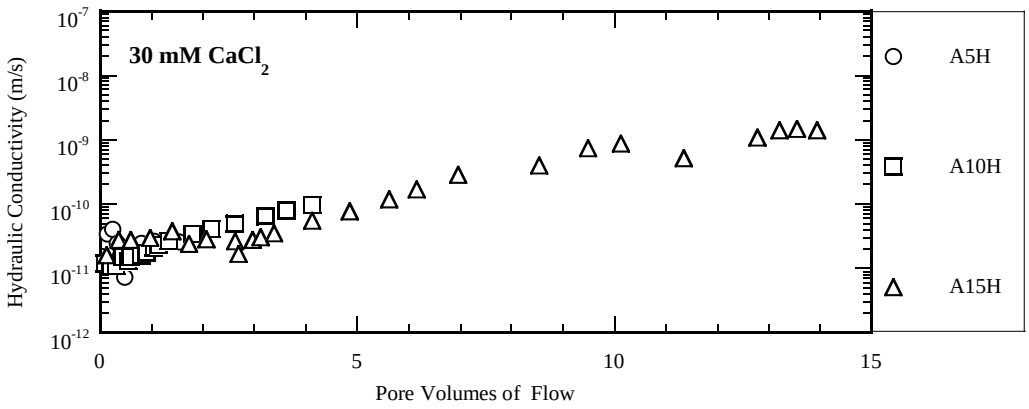

Figure 4.11 Hydraulic conductivity behaviors of GCLs with high MPUA ($M_{b\sim}7$) to 30 mM $CaCl_2$ solution

4.3.3 Hydraulic Conductivity of A-GCLs to 50 mM $CaCl_2$ Solutions

The hydraulic conductivity of M_b~3 to 50 mM $CaCl_2$ solution is shown in Figure 4.12. Due to a testing error, the hydraulic conductivity on A5L to 50 mM $CaCl_2$ solution could not be performed. The initial hydraulic conductivity of A10L and A15L were approximately 2.0×10^{-11} m/s. Although their hydraulic conductivities slightly decreased at the beginning, hydraulic conductivities increased after 3 PVF. Contrary to A-GCLs, the hydraulic conductivity of original L was high (~5.0×10^{-8} m/s) from the beginning till the end of the test. However, the difference between the hydraulic conductivity of artificial and original GCL decreased as the permeation progressed.

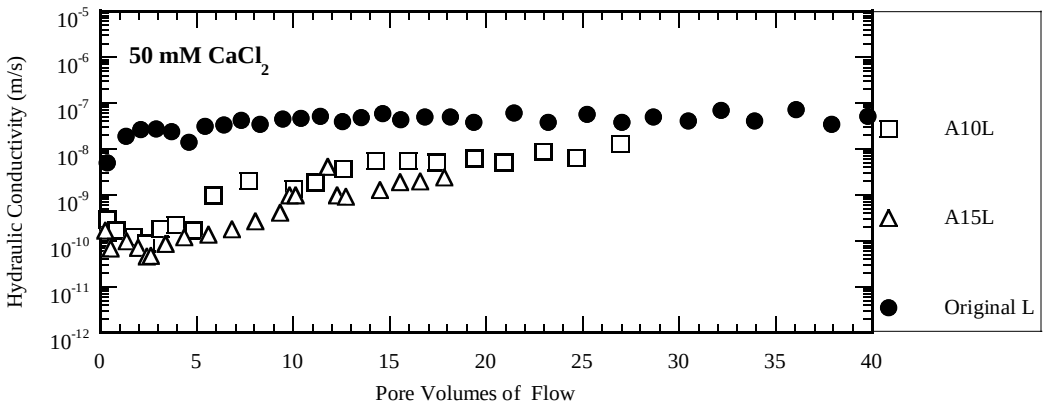

Figure 4.12 Hydraulic conductivity behaviors of GCLs with high MPUA ($M_{b\sim}3$) to 50 mM $CaCl_2$ solution

The results of the hydraulic conductivity to 50 mM $CaCl_2$ solution on the medium MPUA of GCLs is shown in Figure 4.13. The initial hydraulic conductivity of the GCLs was ~1.5×10^{-11} m/s. As can be seen in Figure 4.13, the hydraulic conductivity behaviors of the GCLs showed a behavior similar to those in the experiments with 15 mM and 30 mM $CaCl_2$. However, the upward trend in the hydraulic conductivity values of the GCLs has been observed since the beginning of the experiments. This is due to the fact that the swell index of bentonite is restricted due to abundance of Ca^{2+} ions in the solution (Shackelford 2005).

The hydraulic conductivity of original M reached equilibrium after ~12 PVF, and the final hydraulic conductivity was determined 1.4×10^{-8} m/s. The final hydraulic conductivity of A10M was obtained little greater and was 7.0×10^{-9} m/s at the end of test. However, the tests of A5M and A15M with 50 mM $CaCl_2$ solution are still continuing. Considering the final readings taken, the hydraulic conductivity values of the samples are 6.0×10^{-10} m/s for A5M and 9.3×10^{-11} m/s for A15M. As can be seen in Figure 4.13, the hydraulic conductivity values of both samples tend to increase. When equilibrium is achieved, it is expected that the samples will reach similar values as with original M and A10M.

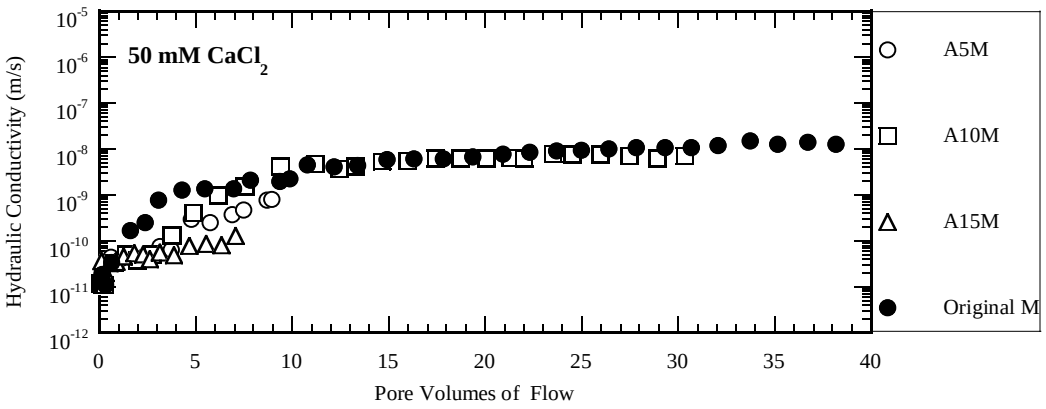

Figure 4.13 Hydraulic conductivity behaviors of GCLs with high MPUA ($M_{b\sim}5$) to 50 mM $CaCl_2$ solution

The hydraulic conductivity behaviors of high MPUA of A-GCLs to 50 mM $CaCl_2$ solutions are given in Figure 4.14. The initial hydraulic conductivities of samples almost the same and were 1.5×10^{-11} m/s. After 1 PVF permeation, the hydraulic conductivities started to increase. Based on the last readings, the hydraulic conductivities of A5H, A10H and A15H were 5.1×10^{-11}, 8.9×10^{-11}, and 1.6×10^{-9} m/s, respectively.

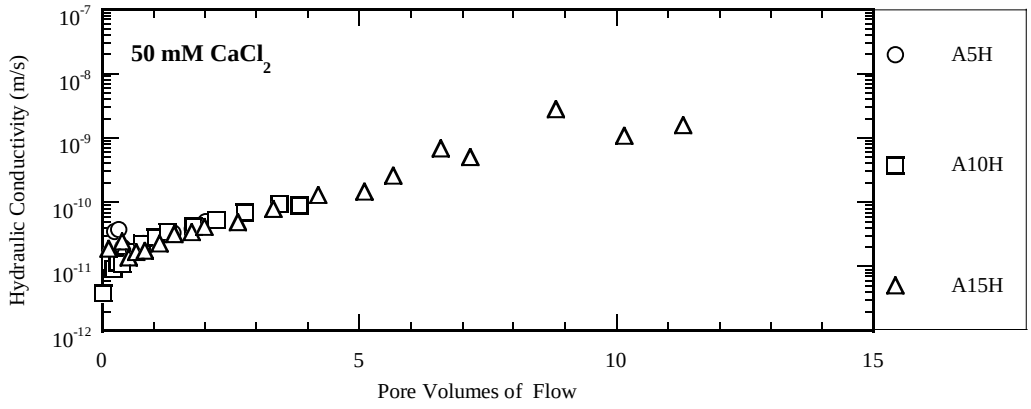

Figure 4.14 Hydraulic conductivity behaviors of GCLs with high MPUA ($M_{b\sim}7$) to 50 mM $CaCl_2$ solution

4.4 Conclusions

The content of this study, the influence of NPD on the hydraulic conductivity behavior was investigated. Laboratory type needle-punching apparatus was designed and produced in order to manufacture GCLs at different NPDs in the laboratory. Thanks to this apparatus, artificial GCLs were manufactured in the laboratory. Then, hydraulic conductivity tests were performed on A-GCLs with different concentrations of $CaCl_2$ solutions. The hydraulic conductivity of A-GCL was compared with the that of original GCL. The findings are summarized below:

A fairly similar behavior was observed between the A-GCLs and the original GCLs, regardless of the concentration of $CaCl_2$ solutions used. The hydraulic conductivity values, which were ~10^{-11} m/s at the beginning, increased slightly during the tests and rose to the levels of ~10^{-8} m/s. This is due to the decrease in the swell index of bentonite as a result of cation replacement of the Ca^{2+} in the $CaCl_2$ solutions and the Na^{+} in the bentonite.

The hydraulic conductivity of the original GCLs was slightly higher than that of the artificial GCLs when 30 mM and 50 mM $CaCl_2$ was used as the permeant. This difference is thought to be due to the higher NPD in the original GCLs compared to A-GCLs.

Since the final hydraulic conductivity values have not been fully obtained due to ongoing tests, it can be claimed that all NPD considered herein can reflect the hydraulic behavior similar to that of original GCL. On the other hand, it was clearly demonstrated by this study that the existence of bundle of fibers, even with low NPD, is responsible for the hydraulic conductivity increase in GCL.

Based on the obtained results and visual inspection made on A-GCLs, the laboratory type needle-punching apparatus is very effective tool to manufacture GCL very close quality to original GCLs manufactured in the factory. Thus, researchers can carry out detailed studies on A-GCLs manufactured with this apparatus.

CHAPTER FIVE
SUMMARY AND CONCLUSIONS

5.1 Conclusions and Recommendations

This study investigates and discusses the influence of MPUA and NPD on GCLs' barrier performance. For this purpose, two types of original GCLs provided by the manufacturer, namely Na-GCL and P-GCL, were subjected to hydraulic conductivity tests. In addition, artificial GCLs were produced with laboratory type needle-punching apparatus to examine the effect of NPD on GCLs' hydraulic conductivity. Based on the obtained results the following conclusions and recommendations can be made:

Conclusions Regarding the Influence of MPUA on GCLs:

- MPUA has a slight effect on the hydraulic conductivity of GCLs when permeated with DIW. That is, the hydraulic conductivity of GCLs slightly changed as the MPUA increased. Due to bentonite's high swell capacity in DIW, the amount of bentonite was not a critical role on hydraulic conductivity.

- Weak $CaCl_2$ solution (6.5 mM) was used only on Na-GCL. The influence of MPUA on these tests, was only seen on M_b3. The hydraulic conductivity of M_b3 was greater than M_b4 and M_b5 from beginning to end of the test. Dye test showed that flow preferentially occurred through bundle of fibers available on M_b3. This behavior suggested that M_b3 (it contains less amount of bentonite) could not swell sufficiently with 6.5 mM $CaCl_2$ and thus the flow passed over the fibers.

- The hydraulic conductivity behavior of GCLs was separated into two parts as initial and final when a medium $CaCl_2$ solution was used (i.e. 15 mM). The influence of MPUA was clearly seen on the initial hydraulic conductivity with both types of GCLs. However, this influence was not observed on the final hydraulic conductivities. It is important to note that MPUA has a critical role on delaying the hydraulic breakthrough (the point where the hydraulic conductivity

started to increase). That is, the higher the MPUA the higher is the PVF observed hydraulic breakthrough.

- When the concentration of $CaCl_2$ in the solution was increased to 30 mM, the influence of MPUA on the initial and final hydraulic conductivity of GCLs was observed obviously. The hydraulic conductivity of M_b3 was greater than M_b4 and M_b5 in both the initial and final.

- The hydraulic conductivity tests to 50 mM $CaCl_2$ solution were conducted only on the P-GCLs. According to the results, the initial hydraulic conductivity of M_b3 was 130 and 240 times greater than that of M_b4 and M_b5, respectively. Also, the influence of MPUA was slightly seen in the final hydraulic conductivities of P-GCLs.

Conclusions Regarding the Coupled Influence of MPUA and $CaCl_2$ Solution on the Final Hydraulic Conductivity of GCLs:

- According to the final hydraulic conductivities of GCLs, generally, increase in the concentration of $CaCl_2$ caused an increase in the hydraulic conductivity.

- Regardless of GCL type, increase in the MPUA caused a slight decrease in the final hydraulic conductivity of GCLs.

Conclusions Regarding the Influence of NPD on the Hydraulic Conductivity of GCLs:

- A similar trend was seen between the A-GCLs and the original GCLs, regardless of the concentration of $CaCl_2$ solutions used.

- Among A-GCLs, the influence of NPD was not observed clearly in terms of hydraulic conductivity. This indicates that increase in the hydraulic conductivity is basically governed by fibers. Fibers can transmit leachate even low NPD. However, this effect is more pronounced when the permeant is different from

water or the solution concentration is equal to or more than 15 mM $CaCl_2$ solution.

- When compared to hydraulic conductivities of original P-GCLs and A-GCLs, although the hydraulic conductivity of the original GCL to 30 mM and 50 mM $CaCl_2$ was relatively higher than A-GCLs, fairly close results were obtained.

- The A-GCLs manufactured with the laboratory type needle-punching apparatus are of a quality that is extremely close to that of original GCLs.

REFERENCES

Anderson, R., Rayhani, M. T., & Rowe, R. K. (2012). Laboratory investigation of GCL hydration from clayey sand subsoil. *Geotextiles and Geomembranes*, *31*, 31–38.

ASTM: D854-10. (2010). Standard Test Methods for Specific Gravity of Soil Solids by Water Pycnometer. *Astm D854*, *C*, 1–7.

ASTM D4318-10. (2005). Standard Test Methods for Liquid Limit, Plastic Limit, and Plasticity Index of Soils. *Report*, *04*, 1–14.

ASTM: D5890-11. (2011). Standard Test Method for Swell Index of Clay Component of Geosynthetic Clay Liners. *ASTM International, West Conshohocken, PA, USA*, *14*, 1–7.

ASTM: D6766-12. (2014). Standard Test Method for Evaluation of Hydraulic Properties of Geosynthetic Clay. *ASTM International, West Conshohocken, PA, USA*, 1–9.

ASTM: D7503-10. (2010). Standard Test Method for Measuring the Exchange Complex and Cation Exchange Capacity of Inorganic Fine-Grained Soils. *ASTM International, West Conshohocken, PA, USA, January*, 1–9.

Benson, C. H., Ören, A. H., & Gates, W. P. (2010). Hydraulic conductivity of two geosynthetic clay liners permeated with a hyperalkaline solution. *Geotextiles and Geomembranes*, *28*(2), 206–218.

Bohnhoff, G. L., & Shackelford, C. D. (2013). Improving membrane performance via bentonite polymer nanocomposite. *Applied Clay Science*, *86*, 83–98.

Chen, J. N., Benson, C. H., & Edil, T. B. (2018). Hydraulic conductivity of geosynthetic clay liners with sodium bentonite to coal combustion product

leachates. *Journal of Geotechnical and Geoenvironmental Engineering*, *144*(3), 04018008.

Di Emidio, G., Mazzieri, F., Verastegui-Flores, R. D., van Impe, W., & Bezuijen, a. (2015). Polymer-treated bentonite clay for chemical-resistant geosynthetic clay liners. *Geosynthetics International*, *22*(1), 125–137.

Guyonnet, D., Gaucher, E., Gaboriau, H., Pons, C.-H., Clinard, C., Norotte, V., & Didier, G. (2005). Geosynthetic clay liner interaction with leachate: Correlation between Permeability, Microstructure, and Surface Chemistry. *Journal of Geotechnical and Geoenvironmental Engineering*, *131*(6), 740–749.

Jo, H. Y., Benson, C. H., & Edil, T. B. (2004). Hydraulic conductivity and cation exchange in non-prehydrated and prehydrated bentonite permeated with weak inorganic salt solutions. *Clays and Clay Minerals*, *52*(6), 661–679.

Jo, H. Y., Benson, C. H., Shackelford, C. D., Lee, J.-M., & Edil, T. B. (2005). Long-term hydraulic conductivity of a geosynthetic clay liner permeated with inorganic salt solutions. *Journal of Geotechnical and Geoenvironmental Engineering*, *131*(4), 405–417.

Jo, H. Y., Katsumi, T., Benson, C. H., & Edil, T. B. (2001). Hydraulic conductivity and swelling of nonprehydrated GCLs permeated with single-species salt solutions. *Journal of Geotechnical and Geoenvironmental Engineering*, *127*(7), 557–567.

Karakuş, Y., Taşkesti, B. E., & Ören, A. H. (2022). Combined influence of subsoil water content and mass per unit area on cation exchange behavior of geosynthetic clay liners. *Geotextiles and Geomembranes*, *50*(1), 174–182.

Katsumi, Takeshi; Ishimori, Hiroyuki; Ogawa, Atsushi; Maruyama, Satoshi, Fukagawa, R. (2008). Effects of water content distribution on hydraulic

conductivity of prehydrated GCLs against calcium chloride solutions. *Soils and Foundations*, *48*(1), 887–896.

Katsumi, T., Ishimori, H., Onikata, M., & Fukagawa, R. (2008). Long-term barrier performance of modified bentonite materials against sodium and calcium permeant solutions, *Geotextiles and Geomembranes*, *26*(1), 14–30.

Koerner, R. M. (2005). *Designing with Geosynthetics*. Pearson Prentice Hall.

Kolstad, D., Benson, C., & Edil, T. (2004). Hydraulic conductivity and swell of nonprehydrated geosynthetic clay liners permeated with multispecies inorganic solutions. *Journal of Geotechnical and Geoenviranmental Engineering*, *130*(12), 1236–1249.

Kolstad, D. C., Benson, C. H., Edil, T. B., & Jo, H. Y. (2004). Hydraulic conductivity of a dense prehydrated GCL permeated with aggressive inorganic solutions. *Geosynthetics International*, *11*(3), 233–241.

Kul, T. O., & Oren, a. H. (2019). Hydration of geosynthetic clay liners (GCLs) on compacted zeolite. *Geosynthetics International*, *26*(1), 81–91.

Lee, J.-M., & Shackelford, C. D. (2005a). Concentration dependency of prehydration effect for a geosynthetics clay liner. *Soils and Foundations*, *45*(4), 27–41.

Lee, J.-M., & Shackelford, C. D. (2005b). Impact of bentonite quality on hydraulic conductivity of geosynthetic clay liners. *Journal of Geotechnical and Geoenvironmental Engineering*, *131*(1), 64–77.

Lee, J.-M., Shackelford, C. D., Benson, C. H., Jo, H.-Y., & Edil, T. B. (2005). Correlating index properties and hydraulic conductivity of geosynthetic clay liners. *Journal of Geotechnical and Geoenvironmental Engineering*, *131*(11), 1319–1329.

Liu, Y., Bouazza, A., Gates, W. P., & Rowe, R. K. (2015). Hydraulic performance of geosynthetic clay liners to sulfuric acid solutions. *Geotextiles and Geomembranes*, *43*(1), 14–23.

Mazzieri, F., di Emidio, G., Fratalocchi, E., di Sante, M., & Pasqualini, E. (2013). Permeation of two GCLs with an acidic metal-rich synthetic leachate. *Geotextiles and Geomembranes*, *40*, 1–11.

Mitchell, J. K. & Soga, K. (2005). *Fundamentals of Soil Behavior*, John Wiley & Sons Inc., New York.

Mendes, M., Touze-Foltz, N., Gardoni, M. d. G., & Mazéas, L. (2014). Diffusion of phenolic compounds through polyethylene films. *Geosynthetics International*, *21*(2), 137–150.

Ören, A. H., & Akar, R. Ç. (2017). Swelling and hydraulic conductivity of bentonites permeated with landfill leachates. *Applied Clay Science*, *142*, 81–89.

Ören, A. H., Taşkesti, B. E., & Özdamar Kul, T. (2022). Evaluating the hydration and hydraulic performance of a geosynthetic clay liner (GCL) in terms of bentonite mass per unit area. *International Journal of Geosynthetics and Ground Engineering*, *8*(2).

Özdamar Kul, T., & Ören, A. H. (2018). Liquid limit based assessment of geosynthetic clay liners subject to hydration and hydraulic conductivity testings. *Geotextiles and Geomembranes*, *46*(June 2017), 436–447.

Petrov, R. J., & Rowe, R. K. (1997). Geosynthetic clay liner (GCL) - chemical compatibility by hydraulic conductivity testing and factors impacting its performance. *Canadian Geotechnical Journal*, *34*(6), 863–885.

Polat, F., Özdamar Kul, T., & Ören, A. H. (2021). Influence of mass per unit area on the hydraulic conductivity of geosynthetic clay liners (GCLs). *European Journal of Science and Technology*, Special Issue 28,1269-1273.

Rayhani, M. T., Rowe, R. K., Brachman, R. W. I., Take, W. A., & Siemens, G. (2011). Factors affecting GCL hydration under isothermal conditions. *Geotextiles and Geomembranes*, *29*(6), 525–533.

Rowe, R. K., Brachman, R. W. I., Hosney, M. S., Take, W. A., & Arnepalli, D. N. (2017). Insight into hydraulic conductivity testing of geosynthetic clay liners (GCLs) exhumed after 5 and 7 years in a cover. *Canadian Geotechnical Journal*, *54*(8), 1118–1138.

Rowe, R. K., Garcia, J. D. D., Brachman, R. W. I., & Hosney, M. S. (2019). Chemical interaction and hydraulic performance of geosynthetic clay liners isothermally hydrated from silty sand subgrade. *Geotextiles and Geomembranes*, *47*(6), 740–754.

Rowe, R. K., & Hamdan, S. (2021). Effect of wet-dry cycles on standard & polymer-amended GCLs in covers subjected to flow over the GCL. *Geotextiles and Geomembranes*, 49(5), 1165–1175.

Rowe, R. K., & Li, T.-K. (2020). Self-healing of circular and slit defects in GCLs upon hydration from silty sand under applied stress. *Geotextiles and Geomembranes*, *48*(5), 667–683.

Ruhl, J. L., & Daniel, D. E. (1997). Geosynthetic clay liners permeated with chemical solutions and leachates. *Journal of Geotechnical and Geoenvironmental Engineering*, *123*(4), 369–381.

Salemi, N., Abtahi, S. M., Rowshanzamir, M., & Hejazi, S. M. (2018). Geosynthetic clay liners: effect of structural properties and additives on hydraulic performance and durability. *Environmental Earth Sciences*, *77*(5), 1–13.

Sarabian, T., & Rayhani, M. T. (2013). Hydration of geosynthetic clay liners from clay subsoil under simulated field conditions. *Waste Management*, *33*(1), 67–73.

Scalia, J., & Benson, C. H. (2010). Preferential flow in geosynthetic clay liners exhumed from final covers with composite barriers. *Canadian Geotechnical Journal*, *47*(10), 1101–1111.

Scalia, J., & Benson, C. H. (2011). Hydraulic conductivity of geosynthetic clay liners exhumed from landfill final covers with composite barriers. *Journal of Geotechnical and Geoenvironmental Engineering*, *137*(1), 1–13.

Scalia, J., Benson, C. H., Bohnhoff, G. L., Edil, T. B., & Shackelford, C. D. (2014). Long-term hydraulic conductivity of a bentonite-polymer composite permeated with aggressive inorganic solutions. *Journal of Geotechnical and Geoenvironmental Engineering*, *140*(3), 04013025.

Setz, M. C., Tian, K., Benson, C. H., & Bradshaw, S. L. (2017). Effect of ammonium on the hydraulic conductivity of geosynthetic clay liners. *Geotextiles and Geomembranes*, *45*(6), 665–673.

Shackelford, C. D., Benson, C. H., Katsumi, T., Edil, T. B., & Lin, L. (2000). Evaluating the hydraulic conductivity of GCL permeated with non-standard liquids. *Geotextiles and Geomembranes*, *18*, 133–161.

Shackelford, C. D., Sevick, G. W., & Eykholt, G. R. (2010). Hydraulic conductivity of geosynthetic clay liners to tailings impoundment solutions. *Geotextiles and Geomembranes*, *28*(2), 149–162.

Tian, K., Benson, C. H., & Likos, W. J. (2016). Hydraulic conductivity of geosynthetic clay liners to low-level radioactive waste leachate. *Journal of Geotechnical and Geoenvironmental Engineering*, *142*(8), 1–12.

Tian, K., Likos, W. J., & Benson, C. H. (2019). Polymer elution and hydraulic conductivity of bentonite–polymer composite geosynthetic clay liners. *Journal of Geotechnical and Geoenvironmental Engineering*, *145*(10), 04019071.

Tong, S., Sample-Lord, K. M., & Bohnhoff, G. L. (2021). Diffusion through sodium and polymer enhanced bentonites exposed to dilute and aggressive solutions. *Canadian Geotechnical Journal*, *58*(5), 603–618.

von Maubeuge, K. P., & Ehrenberg, H. (2014). Investigation of bentonite mass per unit area requirements for Geosynthetic Clay Liners. *10th International Conference on Geosynthetics, ICG 2014, January 2014*.

Wang, B., Xu, J., Chen, B., Dong, X., & Dou, T. (2019). Hydraulic conductivity of geosynthetic clay liners to inorganic waste leachate. *Applied Clay Science*, *168*(August 2018), 244–248.

Wireko, C., & Abichou, T. (2021). Investigating factors influencing polymer elution and the mechanism controlling the chemical compatibility of GCLs containing linear polymers. *Geotextiles and Geomembranes*, *49*(4), 1004–1018.